A STUDY OF WEB WRINKLING DUE TO

ROLLER CURVATURE

By

MATTHEW G. DUVALL

Bachelor of Science
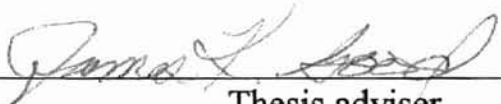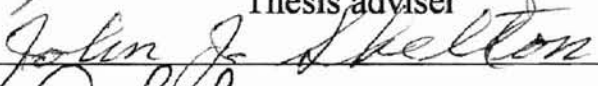
Oklahoma State University
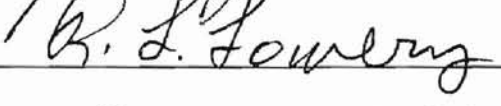
Stillwater, Oklahoma

1994

Submitted to the Faculty of the
Graduate College of the
Oklahoma State University
in partial fulfillment of
the requirements for
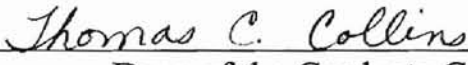the Degree of
MASTER OF SCIENCE
May, 1997

A STUDY OF WEB WRINKLING DUE TO

ROLLER CURVATURE

Thesis Approved:

_____
Thesis adviser

_____

_____

_____
Dean of the Graduate College

PREFACE

This study was conducted to provide insight as to the effect of lateral forces due to roller curvature on webs. As a web travels over a curved axis roller steering effects and lateral forces are imparted to the web. The degree as to which these are present may cause a wrinkle in the web to form. Objectives of this research were to design and build an experimental setup to facilitate examination of Shelton's theoretical buckling model. A deflecting roller was constructed and the deflection profile mathematically modeled. This apparatus was used to test polyester films having a roll width of 6 inches with varying thickness'.

I wish to express my sincere thanks to my advisor, Dr. J.K. Good for his support, guidance, and patience in completion of this work. I also thank Dr. John Shelton and Bruce Feiertag. Without the sharing of expertise and support of these individuals this study would not have been possible. Finally, I wish to thank the School of Mechanical and Aerospace Engineering and the Web Handling Research Center for supporting this study.

TABLE OF CONTENTS

LIST OF TABLES

LIST OF FIGURES

NOMENCLATURE

B	distance between bearings on thin walled roller
C_1, C_2	constants of integration of discontinuity function
a,b,c,d,e	distances from one end of roller to discontinuity points
D_i	inside diameter of thin walled roller
D_o	outside diameter of thin walled roller
E	elastic modulus
E_R	elastic modulus of roller material
E_w	elastic modulus of web material
F	single point load
f	distributed load on roller due to web
f_e	effective distributed load on roller due to web
fpm	feet per minute
g(y)	discontinuity function modeling the roller deflection
I	area moment of inertia
I_R	cross sectional area moment of inertia for thin walled roller
K_1	parabolic approximation constant
k	stiffness of thin walled roller
L	incoming web span length
MRT	Teflon mold release tape

P	point load on a simply supported beam
PET	polyester
R	radius of a thin walled shell
R_1, R_2	reaction forces on a simply supported beam
T	web tension
t	web thickness
v	deflection of a simply supported beam
W	web span width
x	distance along a simply supported beam
y	distance along axis of roller
z	coordinate in direction of roller deflection
δ	spacing between parallel lines along web
ε	lateral strain
ε_y	strain imposed on web due to roller deflection
$\varepsilon_y)_{CR}$	critical buckling strain of a thin walled cylinder
θ_w	angle of web wrap around thin walled roller
$\sigma_y)_{CR}$	critical buckling stress for a thin walled cylinder

I.

Introduction

In the web handling industry, material wrinkling during handling and transportation processes continues to be a source of concern and frustration. Wrinkling can have an important effect on the quality of a web and the quality of a wound roll of web. Wrinkling remains one of the main losses of product quality for most web handling industries. Wrinkling of a web in a material handling process may take on many forms and be due to several causes. It should be noted at this time that a wrinkle is defined as out of plane deformations of a web which are transferred over rollers from one web span to another (1). A web trough is defined as an out of plane deformation that is only present between rollers of a web handling system. Wrinkles themselves may be classified due to the nature of the system and the mechanism of cause. Web wrinkles that form out of alignment with the machine direction are known as shear wrinkles. Wrinkles such as this may be formed due to misaligned rolls, controlled guide rolls, shifting unwind and rewind stands, or interactions between the web and special rollers (curved axis rollers and concave rollers) (1).

All of these occurrences will result in a lateral deformation of the web, which in turn leads to a wrinkle which forms in a direction other than the machine direction. Extensive research of web wrinkling due to misaligned rollers and slack edge phenomena has been completed and is still ongoing. Another class of wrinkle is one which forms in the direction of the material travel, or machine direction. These are cited frequently in the

web handling industry and are noted by obvious troughs in free spans (sections of web material between rollers or handling apparatus) which become wrinkles propagating over rollers in a web handling system, or ultimately see their way to forming corrugations in a final wound roll. Again like shear wrinkles, these may be formed by several different mechanisms such as edge misalignment, roller surface imperfections, or lateral forces imparted to the web span. Upon examination of web handling equipment and web material, one could observe that there are several varying imperfections associated with both items, however relatively uniform and consistent wrinkles form in the material handling process (2).

Given the number of different types of materials which spend part, either brief or extended, or all of their lives in web form, the knowledge as to why these wrinkling phenomena occur and even more importantly what can be done to affect these phenomena is very beneficial to industrialized society. Things such as metals, plastics, papers, and textiles are just a few materials which spend an important portion of their lives in web form. With such a large portion of manufactured materials subject to wrinkling situations the study of these characteristics is quite important. The focus of this study is one which is very specific in the cause of a wrinkled web. The type of wrinkle to be examined in this study is a wrinkle in the machine direction. A wrinkle such as this may be formed due to lateral forces in a free span, lateral steering, or lateral compression of a web. In the first case, lateral forces in a free span, tension in the machine direction between two rollers may cause machine direction out of plane deformations and corrugations in the free span. Given enough severity, this may develop in a corrugation propagating over a roller surface

and forming a wrinkle (3). The second case, lateral steering, may occur when rollers are out of alignment and steering forces are applied to the web. A tape element may be exposed to a steering force which is equal to the buckling force of the web causing a wrinkle to form (4). The case to be studied is case three, lateral compression of the web.

Lateral compressions may be caused by several different methods. They may be caused by a decrease in tension across a driven roller, an increase in temperature of moisture, the bending of a wound roll, or by roller deflection (5). It is with the last case, roller deflection, this study concerns itself with. Roller deflection is apparent in web handling apparatus along with wrinkles and buckles forming at deflected rollers. Rollers may deflect due to high web tension. Rollers may also deflect due to the weight of the web material or the weight of the roller itself. For whatever reason, lateral compression causing wrinkles due to roller deflection is present in the web handling industry and remains a source of headaches and frustration.

The purpose of this study is to examine the current theory of wrinkles formed by lateral compression caused by roller deflection (Shelton) and compare the yieldings of this theory to a controlled experimental apparatus. This apparatus will utilize a web and traverse it over a roller which has the ability to deflect under web tension or an applied external force. This experiment will allow the relationships between web caliper (thickness), web width, web line speed, and degree of curvature of the roller which causes a wrinkle to form to be experimentally verified and explored. While there will be certain limitations to this experiment (i.e. width, speed, and caliper), specific cases of wrinkles occurring were investigated.

II.

Theory of Lateral Compression Caused by Roller Deflection

The theory of lateral compression which this study utilizes is based entirely on Shelton (5). Simply stated it is the deflection of a roller due to web tension or the weight of the roller itself causes a lateral compressive stress in the web. The reason for this compression to occur is the tendency for lanes of the web to become aligned perpendicularly with the roller they are approaching. This occurrence may be seen in figure 1.
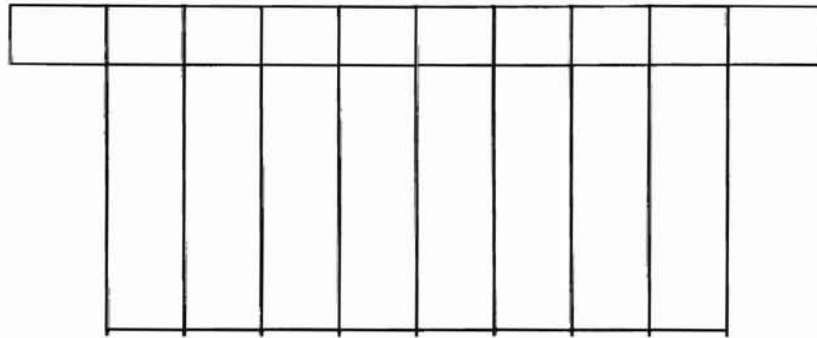
initially perpendicular lanes in span
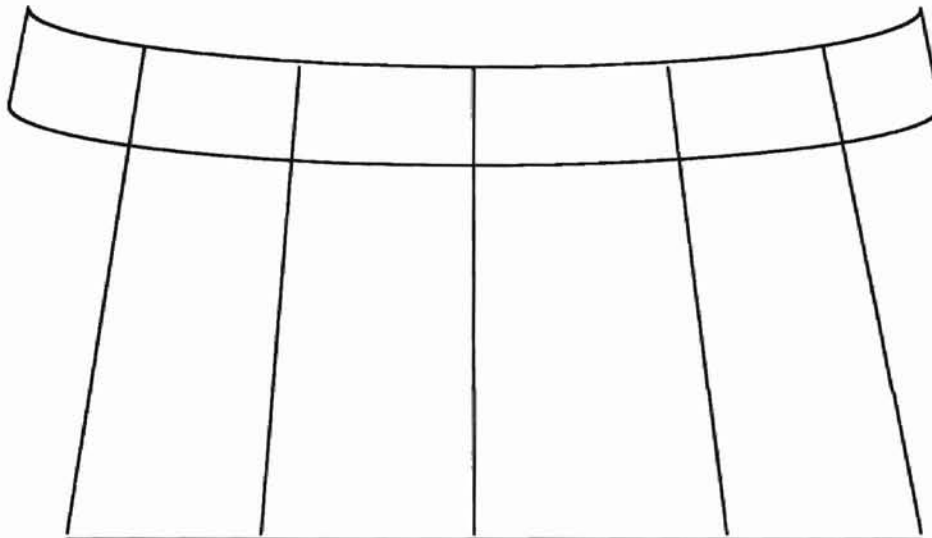
inward directing due to steering effect

figure 1: alignment changes due to roller deflection

As can be seen if figure 1, as develops a certain degree of bow the width of the web lanes

narrow because of the tendency to enter a downstream roller in a perpendicular

orientation. Figure 1 shows the steering which would occur if a web span had zero

compressive strength; that is , the forces resisting lateral compression are neglected (6).

This assumption along with the assumption of perpendicular entry allows for the statement

that compressive forces imparted to the web are due to the kinematic steering effect of the

curved roller. As the web is steered due to the curvature of the roller, the small but not

negligible buckling force of the web is approached. The deflection of the roller is based on

beam theory, modeling the roller as a simply supported beam with a distributed load due

to the web tension, as in figure 2.
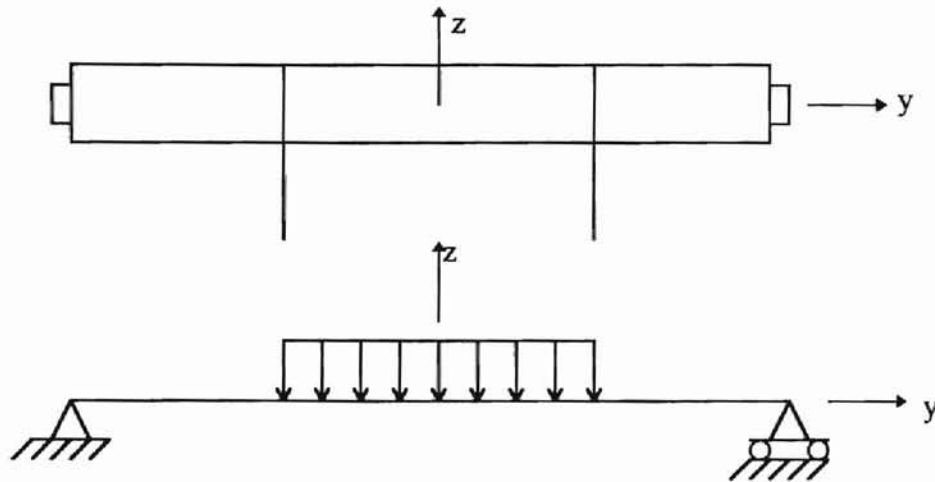
figure 2: deflecting roller model

Shelton makes the assumption in this derivation that even though the deflection curve of

such a beam is never in the shape of a parabola (a single second order term), a parabola is

a reasonable approximation (6). The deflection of the roller is may be approximated by

the equation

6

$$z \approx K_1 y^2, \quad [1]$$

where z is the deflection of the roller relative to the center of the roller, y is the distance

along the roller, and K_1 is a constant (see figure 3).
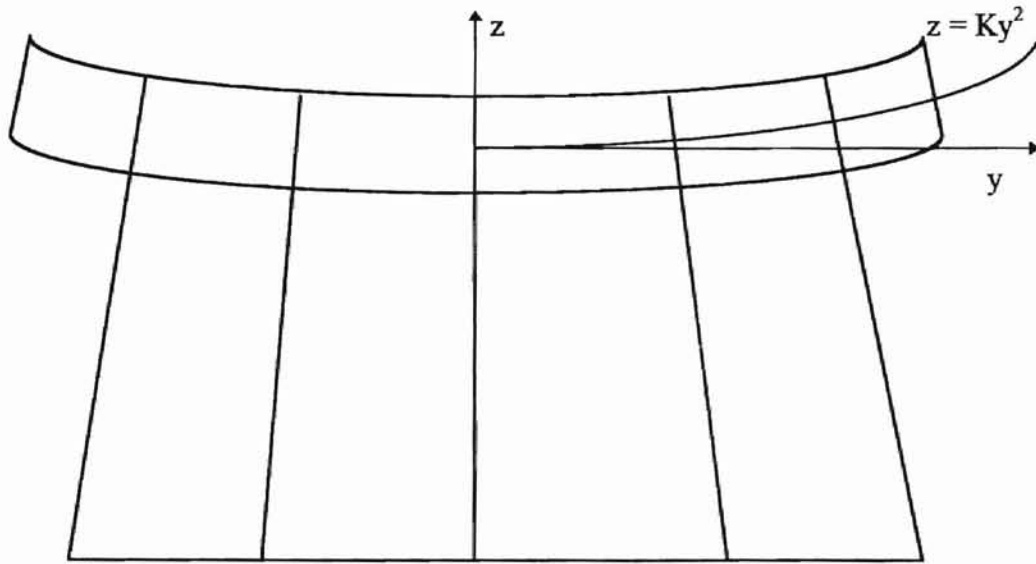
figure 3: parabolic approximation of roller deflection

Lateral compression may be visualized if the entering span is divided into equal width

lanes with parallel lines drawn on the span to separate them. As the roller deflects the web

is assumed to want to approach the roller in a perpendicular fashion. Hence the lanes in

the free span become tapered (figure 3). Because the web is assumed to approach the

bowed web in an angle perpendicular to the roller, the lines drawn to separate the lanes

are rotated through this angle. This angle of rotation will be equal to the slope of the

deflection curve of the roller, or

$$\frac{dz}{dy} = 2K_1 y \qquad [2]$$

Given two points in the web, y_1 and y_2, spaced a distance of Δy apart, the difference in slope between two parallel lines corresponding to these two points is

$$\frac{dz}{dy}_{y2} - \frac{dz}{dy}_{y1} \qquad [3]$$

or

$$2K_1(y_2 - y_1) = 2K_1 \Delta y. \qquad [4]$$

Through the use of some right triangle geometry it can be said that the lateral compression between the two initially parallel lines is

$$\Delta \delta = 2K_1 \Delta y L. \qquad [5]$$

If we now let Δy become W, we can determine the total lateral deformation of the web to be

$$= 2K_1 LW, \qquad [5a]$$

and the lateral strain to be

$$\varepsilon = 2K_1 L. \qquad [6]$$

This strain is constant over the width of the web and based upon assumptions of zero compressive strength and parabolic roller deflection.

As stated earlier the deflection of this roller may be modeled as a simply supported beam. The equation of deflection of this beam for use in Shelton's theory will be derived with the coordinate axes located at the center as in figure 4.

8
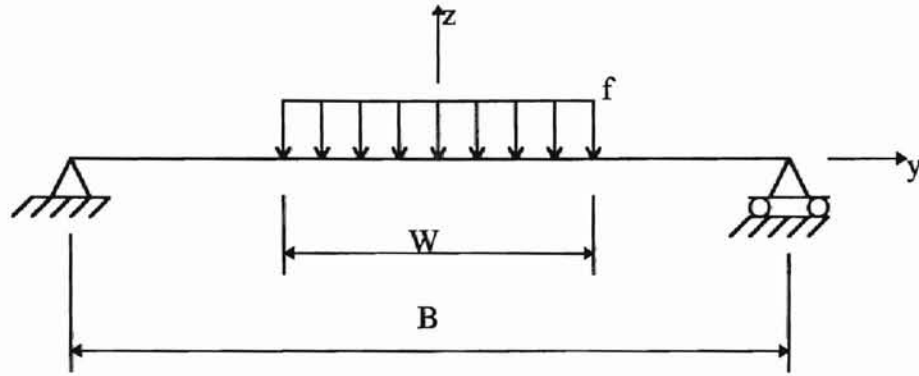
figure 4: location of coordinate axes

The deflection of this beam relative to center is

$$z = \frac{fW^4}{8E_R I_R} \left[\left(\frac{B}{W} - \frac{1}{2} \right)\left(\frac{y}{W} \right)^2 - \frac{1}{3}\left(\frac{y}{W} \right)^4 \right]. \quad [7]$$

Note that in equation 1 z is approximated as a function of y^2 and in equation 7 z is a function of y^2 and y^4. The higher order function is a more reflective model for the deflection of the roller and will be used to establish the constant in equation 6 when the appropriate boundary conditions are applied. The deflection of the edge of the web relative to the center is

$$z_{\frac{W}{2}} = \frac{fW^4}{32E_R I_R} \left(\frac{B}{W} - \frac{7}{12} \right). \quad [8]$$

The slope of the deflection curve is simply the first derivative with respect to y, or

$$\frac{dz}{dy} = \frac{fW^3}{12E_R I_R} \left[3\left(\frac{B}{W} - \frac{1}{2} \right)\left(\frac{y}{W} \right) - 2\left(\frac{y}{W} \right)^3 \right]. \quad [9]$$

9

The slope at the edge of the web is then

$$\frac{dz}{dy}\bigg|_{\frac{w}{2}} = \frac{fW^3}{8E_R I_R}\left(\frac{B}{W} - \frac{2}{3}\right). \quad [10]$$

Equations 7 and 9 are then combined to form an approximation for the conversion of deflection at the web edge to slope at the edge of a web. This relationship is

$$\frac{dz}{dy}\bigg|_{\frac{w}{2}} = -\frac{4z_{\frac{w}{2}}}{W}\left[\frac{\left(\frac{B}{W} - \frac{2}{3}\right)}{\left(\frac{B}{W} - \frac{7}{12}\right)}\right]. \quad [11]$$

By using equilibrium, the distributed force in the z direction on a roller due to tension in the web is

$$f = 2\frac{T}{W}\sin\left(\frac{\theta_w}{2}\right), \quad [12]$$

where T is the web tension, W is the web width, and θ_w is the angle of wrap of the web. Only the component of the angle of deflection which is projected in to the plane of the entering span affects the lateral behavior of the web (9). As can be seen by figure 5, the effective deflection is the actual deflection multiplied by $\sin(\theta_2/2)$. Therefore the effective distributed tensile force on a roller is

$$f_e = 2\frac{T}{W}\sin^2\left(\frac{\theta_w}{2}\right). \quad [13]$$

This may be substituted into equations 6 thru 10.
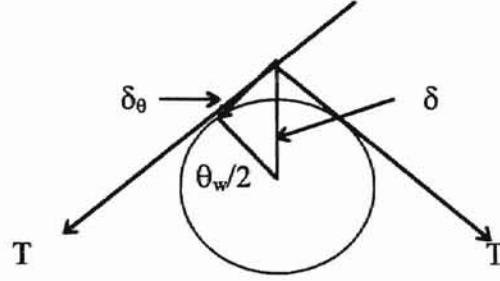
figure 5: Components of roller deflection, δ, which effect web behavior, δ_θ

Expression 1, evaluated at the web edge is

$$z_{\frac{W}{2}} = K_1\left(\frac{W}{2}\right)^2. \quad [14]$$

Solving for K_1 yields

$$K_1 = \frac{4z_{\frac{W}{2}}}{W^2}. \quad [15]$$

By substituting equations 13, 8, and 15 into equation 6, the following relation is developed

$$\varepsilon_y = \frac{LWT}{2E_R I_R}\left(\frac{B}{W} - \frac{7}{12}\right)\sin^2\left(\frac{\theta_W}{2}\right). \quad [16]$$

This is the strain imposed by on the web due to deflection of the roller (10). This derivation does not account for lateral strain in the web as it enters the roller; it is assumed this strain is zero. This strain represents the upper limit of compressive strain caused by the roller deflection due to the fact that the spreading effect of the compressive forces was neglected in the derivation.

Thus, the web traveling over a deflected roller undergoes a compressive cross machine direction strain due to kinematic steering. When this section of web undergoes enough strain a buckle will form. This may be accounted for by modeling the web as a cylindrical shell with an axial load as in figure 6. Timoshenko's theory predicts that a sector of a thin walled cylinder would have the same buckling stress as the complete cylinder. It is also accepted that the pressure caused by web tension would cause the buckling stress to approach the classical prediction.
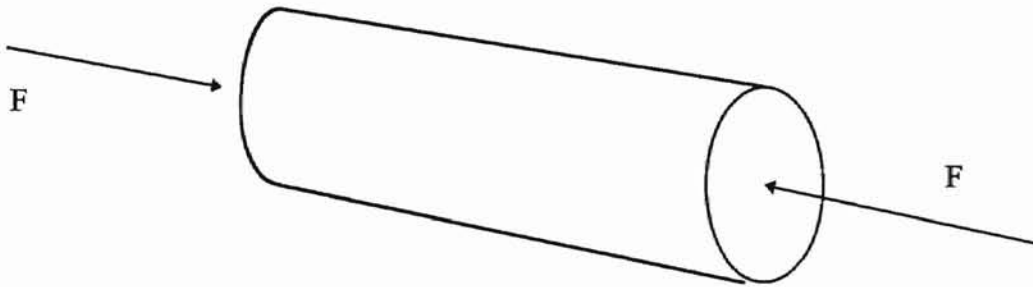
figure 6: cylindrical shell with an axial load

The critical buckling stress for a cylindrical shell with an axial load is (11)

$$\sigma_y)_{CR} \approx 0.605 \frac{E_W t}{R}. \quad [17]$$

Where E_W is Young's modulus of the shell, t is the shell thickness, and R is the radius of the shell. From this relation the buckling strain is

$$\varepsilon_y)_{CR} \approx 0.605 \frac{t}{R}. \quad [18]$$

The strain caused by kinematic steering due to roller deflection can cause a wrinkle only if

its value exceeds that of the critical buckling strain, or in other words

$$\frac{LWT}{2E_R I_R} \left(\frac{B}{W} - \frac{7}{12} \right) \sin^2 \left(\frac{\theta_W}{2} \right) > 0.605 \frac{t}{R}. \quad [19]$$

Buckling in relatively harmless symmetrical corrugations may occur without the formation

of a harmful wrinkle, however. Equation 19 is the inequality defined by Shelton which

should govern web buckling due to roller deflection. This theory of web buckling assumes

that the only strain imparted to web is due to the curvature of the roller, or in other words

kinematic steering effects.

III.

Design of Experimental Setup

The purpose of this experiment was to test Shelton's theory for web buckling due to lateral compressive forces developed due to roller deflection. The challenge was to design a roller which would deflect the amount needed to theoretically cause a wrinkle. The question is then raised, how much deflection is needed to do that? The answer to that question may be deduced from equation 19. It is obvious that material and dimensional properties of the roller must be selected so as to facilitate a wrinkle in a web with given material and dimensional properties while being held at a known web tension, angle of wrap, and incoming web span length. To systematically attack this problem, let's first establish the properties of the web to be used in this experiment. All experimentation will be done using polyester film having a Young's modulus of about 600,000 psi. Film thickness to be tested will range from 18 gauge to 200 gauge (0.00018" to 0.002" thick). The film width to be tested will be 6" to 6 1/2" wide. Next, the capabilities, mainly tension, of the equipment handling the film need to be examined. These experiments will be performed on the "Splicer Winder" located in the Web Handling Research Center laboratory. This machine is capable of generating a maximum web line tension of approximately 20 lb$_f$. This corresponds to roughly 3.33 pli of tension in this case. This is more than sufficient of a tension range to simulate realistic loading situations in the films industry. Due to the nature of this experiment, that being essentially the bowing of a roller, a material must be selected for the roller which does not have an exceedingly high

bending stiffness. The "stiffness" of a material is dictated by two properties, its modulus E and cross-sectional area moment of inertia I. The moment of inertia for an object with a round cross-sectional area, such as a shaft, is

$$I = \frac{\pi}{64} D^4 \quad , \quad [20]$$

where D is the diameter of the shaft. The moment of inertia for a hollow object with a round cross-sectional area, such as a tube, is

$$I = \frac{\pi}{64} \left(D_o{}^4 - D_i{}^4 \right), \quad [21]$$

where D_o is the outside diameter and D_i is the inside diameter of the tube (12). The last dimensional property which needs to be taken into account is the length of the roller. If the roller is to be modeled as a simply supported beam, as in this case, then the relationship between modulus, moment of inertia, and beam length and how these impact bending stiffness may be seen by looking at a very simple case. Look at the simply supported beam with a point load applied directly at its center as in figure 7.
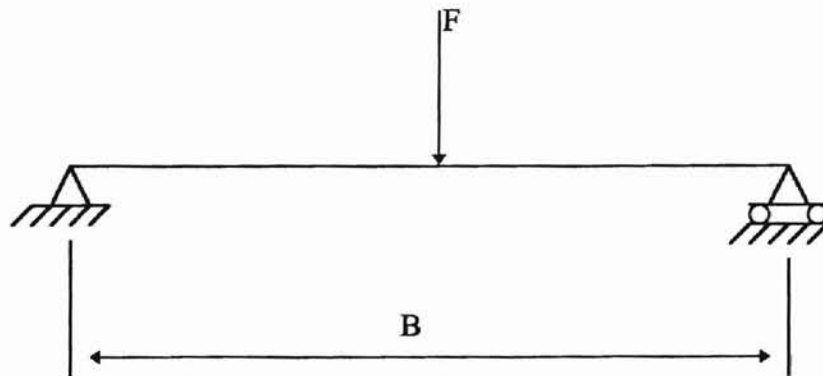
figure 7: simply supported beam with a point load

The equation of deflection for a beam of this type is

$$v = \frac{Px}{48EI}\left(3B^2 - 4x^2\right), \text{ where } 0 \leq x \leq L/2. \quad [22]$$

If the beam is considered merely a "spring" then the spring constant may be found by substituting L/2, where the maximum deflection takes place, for x in equation 22. This yields

$$v = \frac{PB^3}{48EI}. \quad [23]$$

The compliance would then be

$$c = \frac{B^3}{48EI}, \quad [24]$$

and the spring constant, or stiffness, would be

$$k = \frac{1}{c} = \frac{48EI}{B^3}. \quad [25]$$

As can be seen from equation 25 the length of the roller will inversely affect the stiffness of the roller. In other words, the longer the roller the less stiff the roller. The first task in design of the roller is to choose the material. A material with a lower modulus of elasticity is desired for low stiffness behavior. Plastic was considered, however materials such as PVC are not elastic materials and it is speculated that non repeatable testing is possible. A plastic tubing roller may not deflect and return to original configuration. The only logical choice is aluminum having a Young's modulus of around 10,000 ksi (13). Some thin walled aluminum tubing having a wall thickness of 0.025" and an outside diameter of 2.508" was located and purchased. The selection of this material and dimensions leaves only the length of the roller B, the incoming span length L, and the

angle of wrap θ_w to be selected before equation 19 may be applied to see if this design is acceptable. The angle of wrap is selected to be 180°. This angle will impart the largest distributed load to the roller causing the most defection with the least amount of web tension. Also a selection 180° wrap effectively removes the trigonometric portion of equation 19, reducing it to a value of 1. The roller width was established at 18". This was the longest section of the thin walled aluminum tubing as purchased which was straight and the most circular in cross-section. The incoming span length was chosen arbitrarily at 54". When these values are substituted into equation 19 the maximum web thickness allowable for buckling to occur is 0.01". This was 5 times greater than the thickest of the webs to be tested (0.002" thick). Theoretically web buckling should be easily attained with this configuration.

Figure 8 shows the web path on the splicer winder machine for this series of experiments.
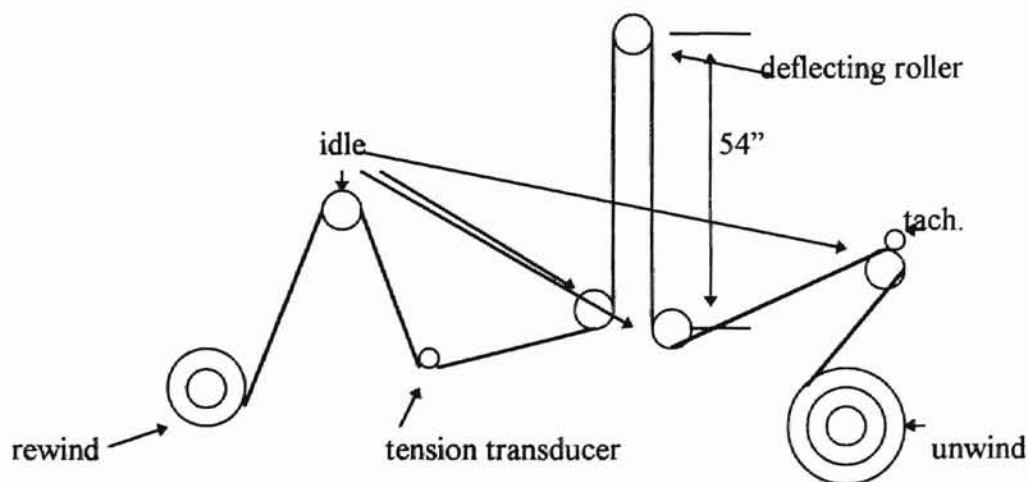
figure 8: web path for this series of experiments

This machine uses a centerwind method with a magnetic hysteretic brake on the unwind. All other rollers are idlers. Constant web line speed is maintained through feedback control. A tachometer is utilized in a feedback circuit to control and maintain the required rewind motor speed during the wind. Web line tension is also controlled through a feedback circuit. A tension transducer is utilized in the circuit to adjust for the required brake current during the unwind. In this experimentation, it is assumed that the tension variations in the free spans due to friction and inertial effects of the idlers may be neglected. All idlers on this machine are made of aluminum shells and have outside diameters of between 3" to 4".

IV.

Initial Experimental Results and Redesign of Roller

The first set of experiments of this study had unexpected results. Buckling was unable to be produced in any of the web calipers available at the time (200, 96, 48 gauge). According to equation 19 the minimum required web tensions required for a buckle to form in the web are 3.677 lb_f, 1.765 lb_f, and 0.882 lb_f for 200, 96, and 48 gauge webs, respectively. All three films were tested with web line tensions up to 20 lb_f and no wrinkles were ever formed. The two questions that must be resolved in this case are what is the required amount of deflection theoretically required to cause wrinkling and does the experimental setup reach this value? The verification if the setup reaches the required amount of deflection and essentially if the mathematical model of the deflecting roller as a simply supported beam is valid is completed relatively easily. A section of the 200 gauge web will be draped over the roller, clamped together, and then used to suspend a 40 lb_f weight (20 lb_f web tension). The deflection of the roller will then be measured at the center and roller end using a dial indicator. This setup may be seen in figure 9. The clamp mass is assumed negligible.
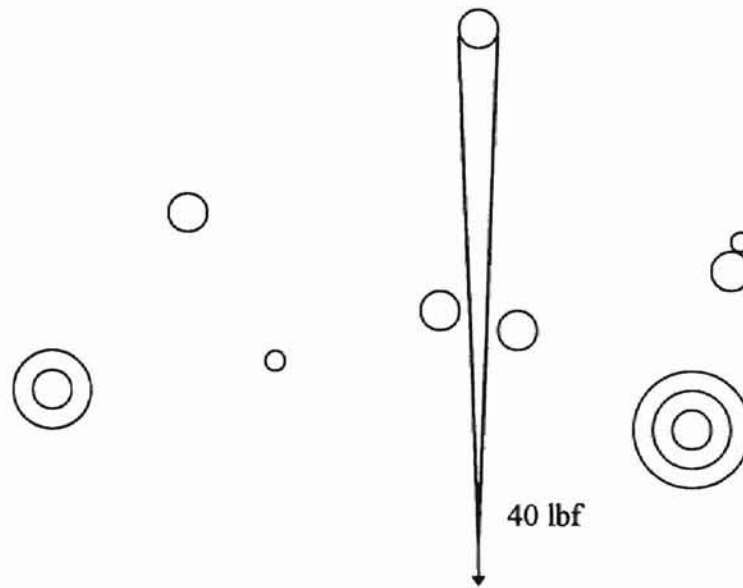
figure 9: roller deflection setup

The theoretical deflections (relative to the supported end of the beam) are 0.0 inches at the

edge and 0.0032 inches at the center. The measured deflections were 0.001 inches at the

roller edge and 0.0045 inches at the center of the web. The deflection of the roller end is

due to shaft effects. That is, the 1" steel passive shaft which supports the roller is

deflecting slightly also. This deflection may be subtracted out making all measurements

relative to the roller end. The measured deflections are then 0.0 inches at the end and

0.0035 inches at the center. This is under a 10% difference, and also proves that the

modeling of the deflecting roller as a simply supported beam is valid. The assumption that

the roller bearings in the end of the roller have enough freedom that rotation at the

supports is unrestrained and thus the roller behaves as a simply supported beam is valid.

This study takes on an interesting twist at this point. It appears that all the theory utilized to develop this experimental test is not valid, at least for the case examined (6" width w/ 54" entrance span). The roller deflects as predicted for a known distributed load applied to it, and yet no buckle forms for the extremely low web tensions theoretically required to cause them. In addition, no wrinkle will form even when the applied load is over 20 times the required load. The above development causes this study to focus on a new question. How much deflection is required to cause the buckling? To experimentally explore the possibilities, the experimental setup must be redesigned to allow for roller curvature to be variable in the course of the experiment. The mechanism chosen to facilitate this is to place two dead loads on either side of the web. The curvature of the roller in this case is not the only resultant of the distributed load of the web but also the added applied forces. In this fashion, the web tension may be held constant, but curvature of the roller changed throughout the experiment. The new load configuration may be seen in figure 10.
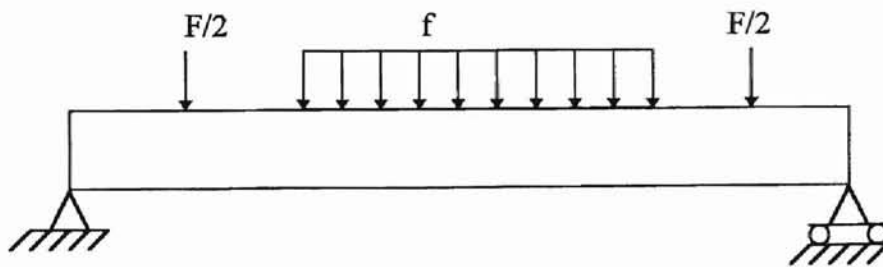

figure 10: new load configuration

To incorporate this loading into the setup, two 1" wide spherical self aligning roller bearings will be placed on both sides of the web area. The center lines of the bearings will each be located 5" from the ends of the roller. Aluminum plates were then machined to fit around the bearings and allow for a cross bar to be installed where the load will be applied in the center, equally distributing half of the load to each bearing, as in figure 11.
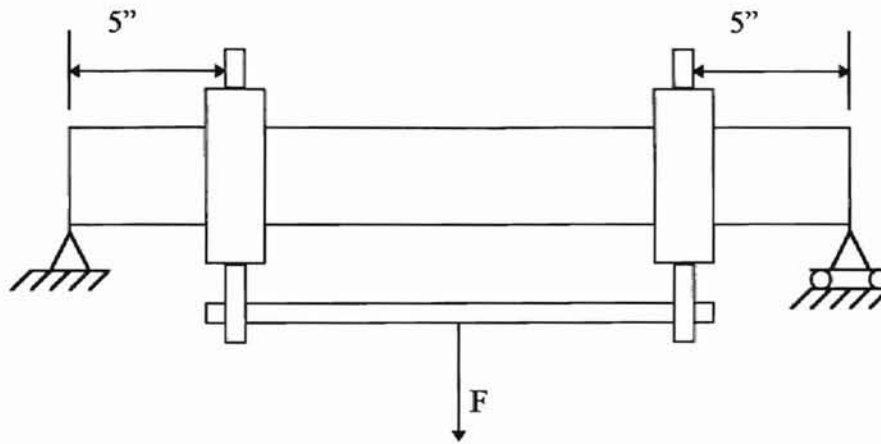
figure 11: bearing and load plate assembly

The cross bar may then be connected to a cable and pneumatic cylinder directly below to actuate the applied dead force. A pressure regulator on the supply air of the cylinder is used to allow for a variable applied load. To measure the applied force, a Measurements Group transducer is placed between the cable and cylinder. This new setup allows for the curvature of the roller to be adjusted to the point where a wrinkle forms and thus the curvature required to cause a wrinkle may be found. The new experimental setup may be seen in figure 12.
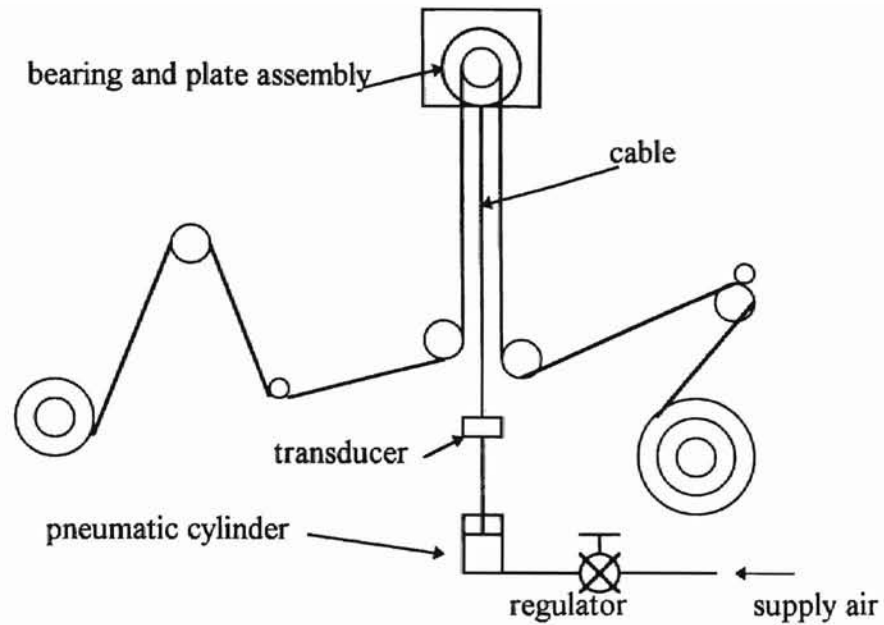
figure 12: load cylinder setup

The roller may still be modeled as a simply supported beam, however a new

deflection equation must be derived to account for the added loads. The new beam

configuration is seen in figure 13.
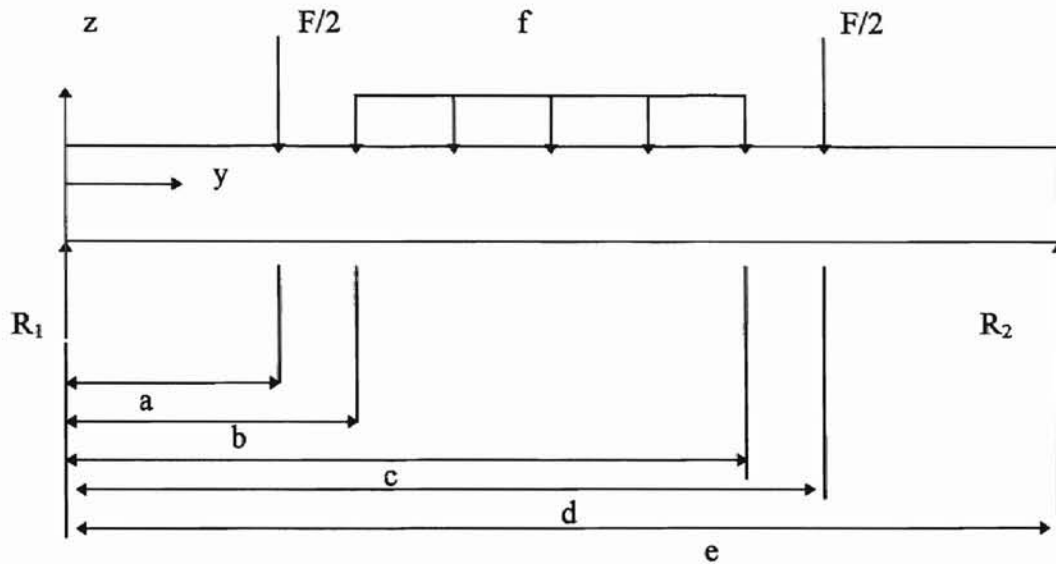
figure 13: beam configuration for new loads

The reaction forces R_1 and R_2 may be found by a summation of forces on the roller. For the force summation the distributed load may be simplified to a single point load, F (see figure 14).

figure 14: Simplified loading of roller

Summing forces equal to zero yields

$$R_1 + R_2 - F - P = 0 \quad [26]$$

or

$$R_1 + R_2 = fW + F. \quad [27]$$

Through symmetry we may say that

$$R_1 = R_2, \quad [28]$$

therefore

$$R_1 = R_2 = f\frac{W}{2} + \frac{F}{2}. \quad [29]$$

The deflection curve of a simply supported beam with this type of loading may be solved

by using discontinuity functions (7). With the reaction forces and applied dead loads
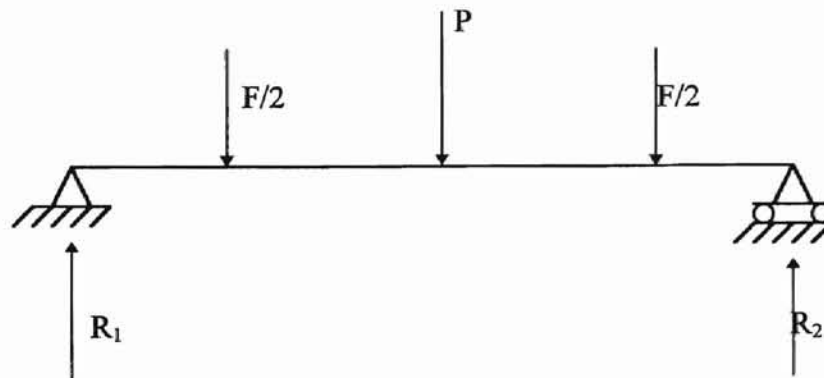
represented as point loads R_1, R_2, and $F/2$ and the load due to web tension as a distributed

force f (see figure 13), the following discontinuity function may be written

$$g(y) = -R_1 <y>^{-1} + \frac{F}{2} <y-a>^{-1} + f(<y-b>^0 - <y-c>^0) + \frac{F}{2} <y-d>^{-1} - R_2 <y-e>^{-1}.$$
$$[30]$$

Because the method of discontinuity functions only allows the individual load functions to

be non-zero if the bracketed value is positive, the term $R_2<y-e>^{-1}$ may be ignored because

the distance y along the roller is never greater than e the roller's total length. Thus the

discontinuity function simplifies to

$$g(y) = -R_1 <y>^{-1} + \frac{F}{2} <y-a>^{-1} + f(<y-b>^0 - <y-c>^0) + \frac{F}{2} <y-d>^{-1}. \quad [31]$$

Through the use of the differential equation of beam deflection, the following relation may

be stated

25

$$EIv'''' = g(y) = -R_1 <y>^{-1} + \frac{F}{2} <y-a>^{-1} + f(<y-b>^0 - <y-c>^0) + \frac{F}{2} <y-d>^{-1}.$$

[32]

Once this is established, we may integrate twice obtaining

$$EIv''' = -V = -R_1 <y>^0 + \frac{F}{2} <y-a>^0 + f <y-b>^1 - f <y-c>^1 + \frac{F}{2} <y-d>^0$$

[33]

and

$$EIv'' = -M = -R_1 y + \frac{F}{2} <y-a>^1 + \frac{f}{2} <y-b>^2 - \frac{f}{2} <y-c>^2 + \frac{F}{2} <y-d>^1. \quad [34]$$

Because we began with the complete expression for g(y) including the reaction forces, no

constants of integration are required to find the shear and moment forms (8). Integrating

two more times to obtain the equation of deflection yields

$$EIv' = -\frac{R_1}{2} y^2 + \frac{F}{4} <y-a>^2 + \frac{f}{6} <y-b>^3 - \frac{f}{6} <y-c>^3 + \frac{F}{4} <y-d>^2 + C_1 \quad [35]$$

and

$$EIv = -\frac{R_1}{6} y^3 + \frac{F}{12} <y-a>^3 + \frac{f}{24} <y-b>^4 - \frac{f}{24} <y-c>^4 + \frac{F}{12} <y-d>^3 + C_1 y + C_2.$$

[36]

Note that for the slope and deflection forms evaluation of constants of integration is

required. The boundary conditions for a simply supported beam are

$$v(0)=0 \quad \text{and} \quad v(e)=0. \quad [37]$$

Application of these boundary conditions to equations 35 and 36 enables the solving of the

constants C_1 and C_2 as follows,

$$C_1 = \frac{f}{24} \frac{(e-c)^4}{e} + \frac{R_1}{6} e^2 - \frac{f}{24} \frac{(e-b)^4}{e} - \frac{F}{12} \frac{(e-a)^3}{e} - \frac{F}{12} \frac{(e-d)^3}{e} \quad [38]$$

and

$$C_2 = 0. \quad [39]$$

If symmetry is applied then an analysis of only 1/2 of the roller is required allowing for the elimination of the <y-c> and <y-d> terms in equation 36. Substitution of the constants of integration back into equation 36 yields the final form of the roller deflection equation

$$EIv = -\frac{R_1}{6}y^3 + \frac{F}{12}<y-a>^3 + \frac{f}{24}<y-b>^4 + C_1y. \quad [40]$$

Once again realize that the second and third terms of equation 16 have a non-zero value only when the contents inside the discontinuity brackets yield a positive result. Therefore,

$$EIv = -\frac{R_1}{6}y^3 + C_1y \text{ for } (y \le a), \quad [41]$$

$$EIv = -\frac{R_1}{6}y^3 + \frac{F}{12}(y-a)^3 + C_1y \text{ for } (a < y \le b), \quad [42]$$

and

$$EIv = -\frac{R_1}{6}y^3 + \frac{F}{12}(y-a)^3 + \frac{f}{24}(y-b)^4 + C_1y \text{ for } (b < y \le c). \quad [43]$$

The relationships 41, 42, and 43 are the roller deflection relative to the end of the roller. The theory derived by Shelton uses a deflection equation relative to the center of the roller. These relationships may be easily incorporated into Shelton's theory by the following relation

$$EIv(y)_{rel\_cent} = EIv\left(\frac{e}{2}\right) - EIv(y). \quad [44]$$

The sign of this relation simply dictates the direction of the deflection. As in the case where no dummy loads were applied, the actual deflection must be experimentally verified to assure that the deflection equation for this case is valid. The test of the deflection of

the roller will only be performed in the region of web contact. Deflection at the center of the roller and at 1" increments off of center will be measured. The range of applied forces to be tested will be 50 lb_f to 230 lb_f. Only 1/2 of the 6" web area needs to be tested, however symmetry will be verified. It should be noted that the weight of the bearings, shoulder plates, and cross bar has been taken into account and added in to the applied dead load but this weight is so small (10.3 lb_f) it could probably be ignored. For the purposes of the deflection test, it will be ignored. Because the first experiment was unsuccessful in making a buckle, the question of slippage was asked. Could it be a case where the film slipped enough on the roller so as its longitudinal stiffness did not allow for a wrinkle to form? The surfaces of contact in the first experiment was polyester on aluminum. In addition, a set of experiments will be performed with a "mold release tape" with a Teflon type surface will be used. This material has an almost cohesive attraction to polyester, and will allow for the assumption of no slippage to be made The coefficient of friction between these surfaces will be tested utilizing the COF testing apparatus in the Web Handling Research Center. In addition to the new surface, a broader range of web thickness will be evaluated.

V.

Experimental Results

The results of the second batch of experiments were quite exciting. Wrinkles were formed on several different calipers of film. While wrinkles did not form on all web thickness', enough data and successful points were taken to form a correlation. While the formation of wrinkles is the primary focus of this study, the analysis of the deflection of the roller with the new load geometry must be addressed first.

The analysis of the roller deflection is needed where the web is in contact with the roller. Or, in other words, only the center 6" of the roller. It is in this section where the deflection and slope is critical because it is in direct contact with the film. The deflections of the roller were measured with a proximity probe which can register distance changes as small as 0.1 mils (0.0001"). Measurements were taken at the center of the roller (designated as Y0) and at 1 inch increments off of center (designated as Y1, Y2, and Y3 respectively). Points along the entire 6" web length were examined to verify symmetry. It was discovered that the deflection is in fact symmetrical. Because of symmetry it is only necessary to display data from one half of the roller area in contact with the web. Raw data points are measurements of deflections relative to the shaft support frame which bolts the roller assembly to the winding machine. To remain in agreement with Shelton's theory the deflection relative to the center of the roller must be known. This may be found with relationships similar to equation 44, or

$$y_{0relative} = 0, \quad [45]$$

$$y_{1relative} = y_0 - y_1, \quad [46]$$

$$y_{2relative} = y_0 - y_2, \quad [47]$$

and

$$y_{3relative} = y_0 - y_3. \quad [48]$$

The subscript indicates the distance from the center of the roller. The raw data deflection

points and the calculated deflection points relative to center are available in table 1.

Table 1

Raw data points and calculated deflections relative to center of roller

applied force	Deflection							
(lbf)	Y0 (mil)	Y1 (mil)	Y2 (mil)	Y3 (mil)	Y0rel (mil)	Y1rel (mil)	Y2rel (mil)	Y3rel (mil)
0	0	0	0	0	0	0	0	0
50	4.7	4.6	4.4	4.2	0	0.1	0.3	0.5
60	5.6	5.5	5.3	5.1	0	0.1	0.3	0.5
70	6.6	6.5	6.2	5.9	0	0.1	0.4	0.7
80	7.5	7.4	7.2	6.8	0	0.1	0.3	0.7
90	8.5	8.4	8.1	7.6	0	0.1	0.4	0.9
100	9.4	9.3	9	8.5	0	0.1	0.4	0.9
110	10.3	10.2	9.9	9.4	0	0.1	0.4	0.9
120	11.3	11.2	10.8	10.3	0	0.1	0.5	1
130	12.3	12.1	11.7	11.2	0	0.2	0.6	1.1
140	13.2	13	12.6	12	0	0.2	0.6	1.2
150	14.1	14	13.5	12.9	0	0.1	0.6	1.2
160	15	14.9	14.4	13.7	0	0.1	0.6	1.3
170	15.9	15.8	15.3	14.6	0	0.1	0.6	1.3
180	16.8	16.7	16.2	15.4	0	0.1	0.6	1.4
190	17.8	17.7	17.1	16.3	0	0.1	0.7	1.5
200	18.7	18.6	18	17.1	0	0.1	0.7	1.6
210	19.6	19.5	18.9	17.9	0	0.1	0.7	1.7
220	20.5	20.4	19.7	18.8	0	0.1	0.8	1.7
230	21.4	21.3	20.6	19.6	0	0.1	0.8	1.8

As can be seen from table 1 the limited resolution of the proximity probe does present a problem when trying to measure deflections on this magnitude. The deflection value located 1" from center should really require an instrument of greater sensitivity. Equation 44 may be utilized to calculate the theoretical deflection relative to the center of the roller. By substituting in the applied force, removing the distributed load because there was no tensioned film used for these tests, and dividing through by the EI term the deflection may be calculated. Table 2 displays the calculated theoretical deflections and the difference between the experimentally measured values.

Table 2

Theoretical deflections relative to center and differences from experimental values

applied force	Deflection							
(lbf)	Y0rel (mil)	Y1rel (mil)	Y2rel (mil)	Y3rel (mil)	difference between theo. and exp. (mil)			
0	0	0	0	0	0	0	0	0
50	0	0.042	0.166	0.374	0	-0.058	-0.134	-0.126
60	0	0.05	0.2	0.449	0	-0.05	-0.1	-0.051
70	0	0.058	0.233	0.524	0	-0.042	-0.167	-0.176
80	0	0.067	0.266	0.599	0	-0.033	-0.034	-0.101
90	0	0.075	0.299	0.674	0	-0.025	-0.101	-0.226
100	0	0.083	0.333	0.748	0	-0.017	-0.067	-0.152
110	0	0.091	0.366	0.823	0	-0.009	-0.034	-0.077
120	0	0.1	0.399	0.898	0	-1.4E-15	-0.101	-0.102
130	0	0.108	0.432	0.973	0	-0.092	-0.168	-0.127
140	0	0.116	0.466	1.048	0	-0.084	-0.134	-0.152
150	0	0.125	0.499	1.123	0	0.025	-0.101	-0.077
160	0	0.133	0.532	1.198	0	0.033	-0.068	-0.102
170	0	0.141	0.566	1.272	0	0.041	-0.034	-0.028
180	0	0.15	0.599	1.347	0	0.05	-0.001	-0.053
190	0	0.158	0.632	1.422	0	0.058	-0.068	-0.078
200	0	0.166	0.665	1.497	0	0.066	-0.035	-0.103
210	0	0.175	0.699	1.572	0	0.075	-0.001	-0.128
220	0	0.183	0.732	1.647	0	0.083	-0.068	-0.053
230	0	0.191	0.765	1.721	0	0.091	-0.035	-0.079

As can be seen from the charts the theoretical values are generally less than the experimental deflection values. However, the largest difference between experimental and theoretical is -0.23 mils (-0.00023"). This error is small and is believed to be due to the inductance probe possibly not having a small enough resolution (the smallest increment of Δy measurable is 0.1 mil). The process of subtracting all deflection measurements from the center deflection and the limited measurement precision for deflections of these small magnitudes could have caused this error. The results of these tests do prove what was expected. First, the roller deflection is symmetric about its center and is, for practical purposes, a parabola. Second, the derived equation of deflection is sufficiently accurate. It will be assumed through the rest of this study that this equation represents the true deflection of the roller.

The second step of this set of experimentation is to measure the coefficient of friction between the roller surface and the polyester film used in the tests. To accomplish this task the coefficient of friction testing apparatus in the Web Handling Research Laboratory was used. Table 3 shows the results of this testing.

Table 3

Coefficients of friction between roller surfaces and polyester film

	Aluminum Surface	Mold Release Tape Surface
Static Coefficient	0.3	1.7
Kinetic Coefficient	0.2	1.6

As can be seen from the above table the static coefficient of friction between the PET and aluminum is a typical value of around 0.3. However the coefficient between the MRT and PET surface is greater than one, indicating an actual cohesive effect between the two surfaces. While slippage may possibly occur between the aluminum and PET surfaces, it will be assumed through the rest of this study that there is no slippage between the MRT and PET in these experiments.

Two aspects of these experiments have now been addressed. The first is the accuracy of the deflection equation, and the second is the coefficient of friction between the roller surfaces and the polyester film. The final and perhaps the most important focus of this study will be addressed now. Wrinkles were able to be formed in this set of experiments, however as stated before they were not able to be formed with the conditions prescribed by the theory of Shelton. There were essentially 2 different types of experiments performed. The first evaluated the amount of dead force applied to cause a wrinkle or hard crease to form. The second evaluated the amount of dead force applied to bring the film to a state of impending wrinkle, or in other words a wrinkle that is just beginning to form or cannot remain set in the film. In both conditions, status of the wrinkle (either impending or set in the film) were judged by the experimenter at the time.

No standard or clear division defining impending or set wrinkle exists so the best judgment was used. An impending wrinkle is judged as one which could not remain in the film. When a required deflection point is reached an impending wrinkle will "pop" in and "pop" out of the film. A set wrinkle is one which forms and stays in the film. The method

of taking data is simple. Set the winding machine at a known web speed and line tension and deflect the roller until a wrinkle forms. Tests were performed on both surface types however most data is taken with the mold release tape surface due to the fact that the no slipping assumption appears to be more valid for this setup. For the case of PET on aluminum, figure 15 shows the results for one test. As can be seen from figure 15, the amount of force required to cause the wrinkle appears to level out and be somewhat constant above around 150 fpm. The area below 150 fpm appeared to be an area of concern so another test was run to verify the "decay look" of the profile. It appears that the lower the web speed the greater the required force to cause a wrinkle. Another test was performed with web speeds ranging between 50 and 250 fpm. These results may be seen in figure 16. As can be seen in figure 16, the higher force applied to the roller at lower tensions was repeated for this test. The lower the line speed, the more curvature required for a wrinkle to form. It is at this time that the question of film slippage on the roller surface is considered. It is believed that this may be the cause of the behavior at the lower line speeds.
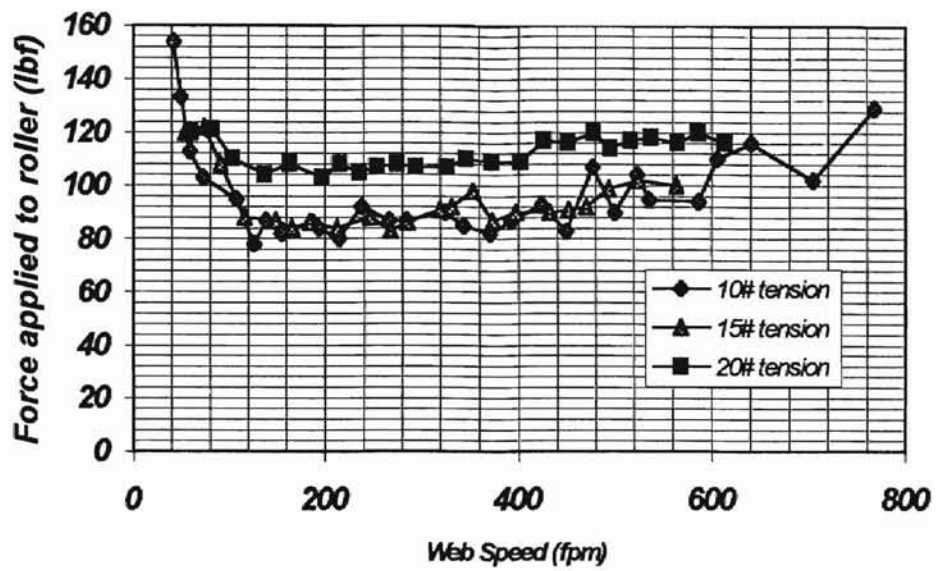
figure 15: Force applied to roller to induce wrinkle vs. Web speed (48 gauge web, PET on aluminum)
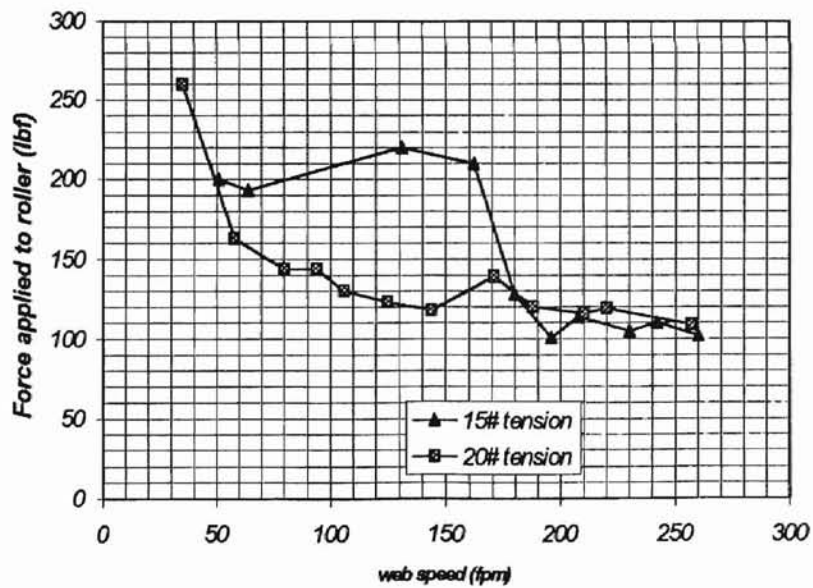
figure 16: Dead force applied to roller to induce wrinkle vs. web speed (48 gauge web, PET on aluminum)

35

From this point forward all experiments will be performed on a mold release tape and PET surface. Re-performing the test which generated figure 15 yields the results which may be seen in figure 17.
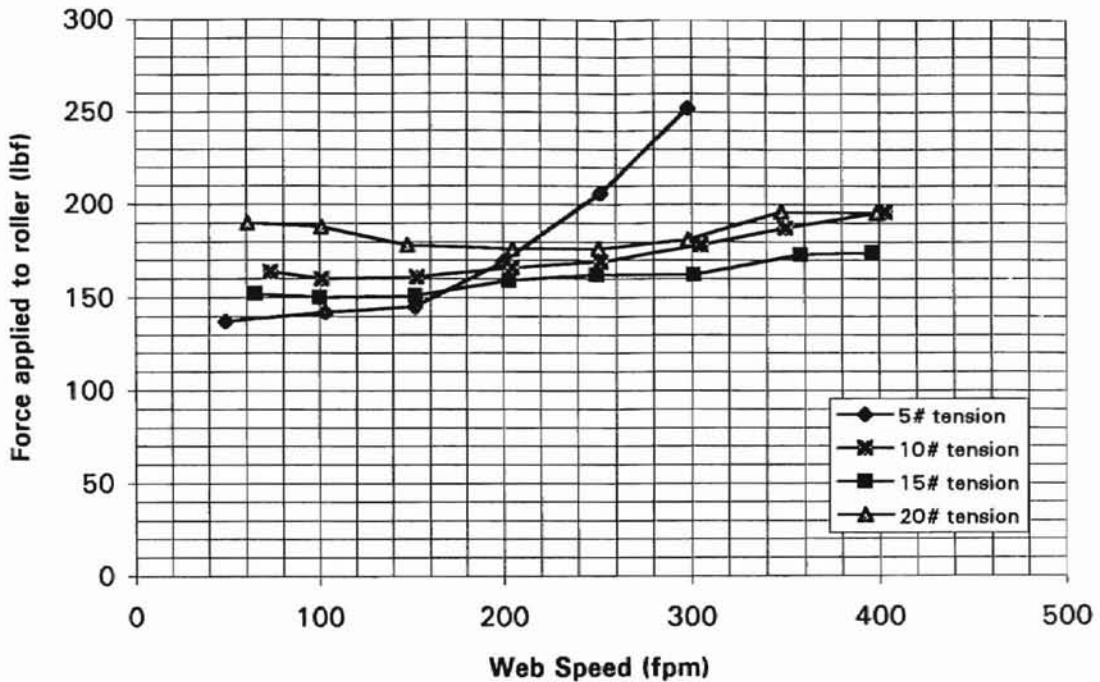

figure 17: Dead Force Applied to Roller to Induce Wrinkle Vs. Web Speed (48 gauge web, PET on MRT)

As can be seen from figure 17 the test did not behave the same in the lower line speed region. The curves of required load, and essentially deflection, are extremely flat and for all purposes constant. The only curve in this case which behaves quite differently is the 5 lb$_f$ tension curve. During the course of the 5 lb$_f$ tension test, the film did slip on the roller. Due to the effects of the applied load the film could not turn the roller with this low line tension. Even though spherical self aligning bearings were used there is still a torsional

load instilled on the roller as it deflects. If the tension in the web is not great enough to give enough surface traction between the film and the roller to overcome this increase torsional load, the film motion cannot turn the roller. Slipping will occur at this point and a wrinkle cannot be maintained in the film. The rest of the tests to find the formation of a hard wrinkle or crease will be carried out in the same manner on different web gages, and the results of these tests are available in figures 18, 19, 20, and 21.
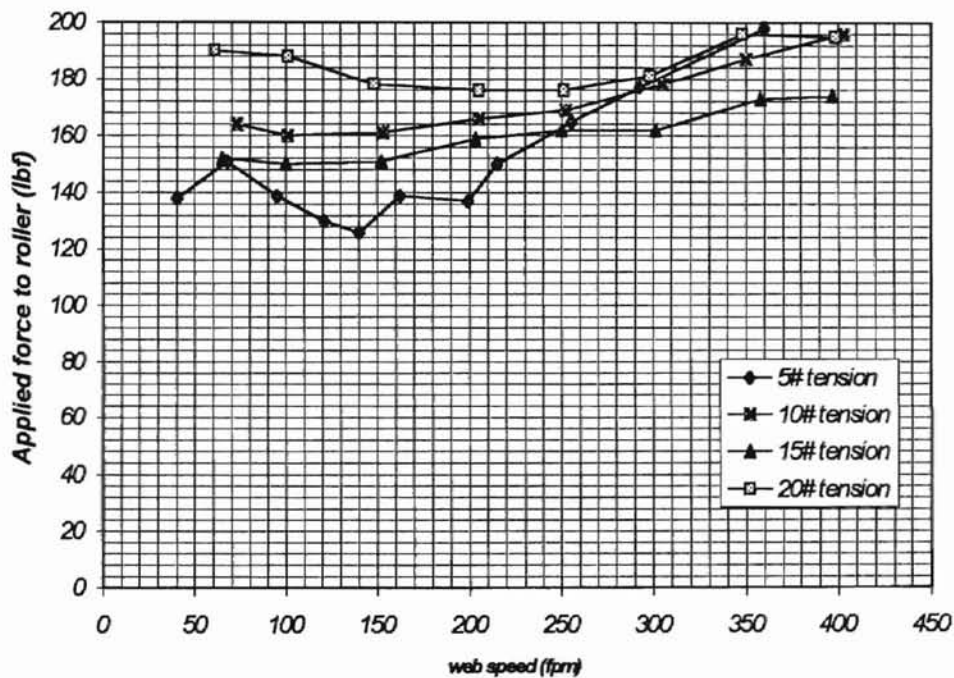
figure 18: Applied Force to cause Hard Crease Vs. Web Speed (56 gauge, PET on MRT)
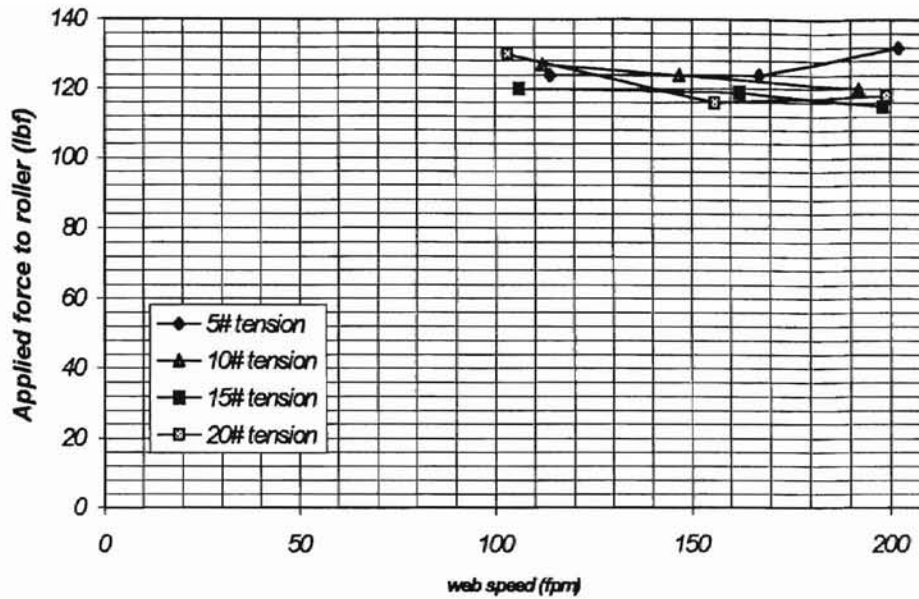
figure 19: Applied Force to Cause Hard Crease Vs. Web Speed (38 gauge, PET on MRT)
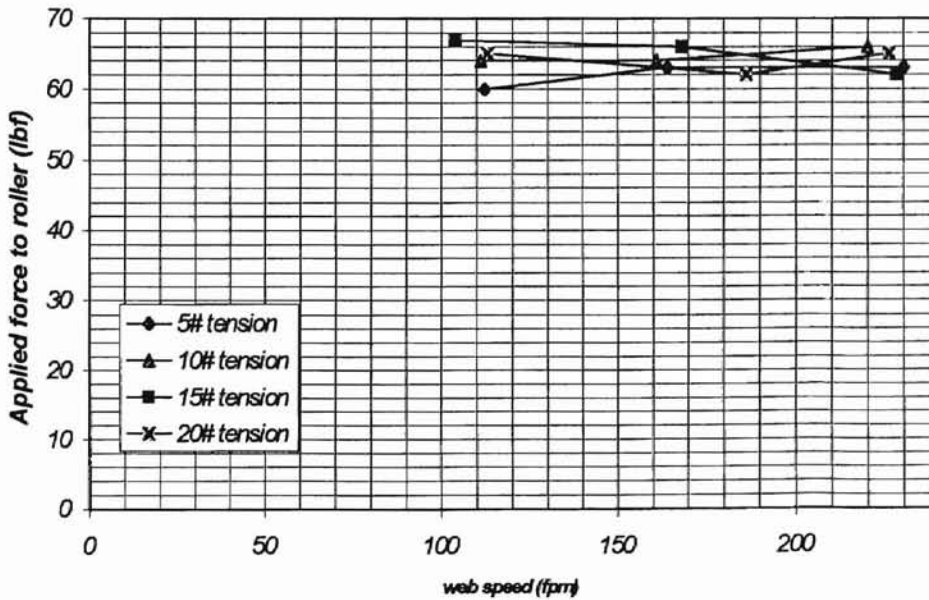
Figure 20: Applied Force to Cause Hard Crease Vs. Web Speed (26 gauge, PET on MRT)
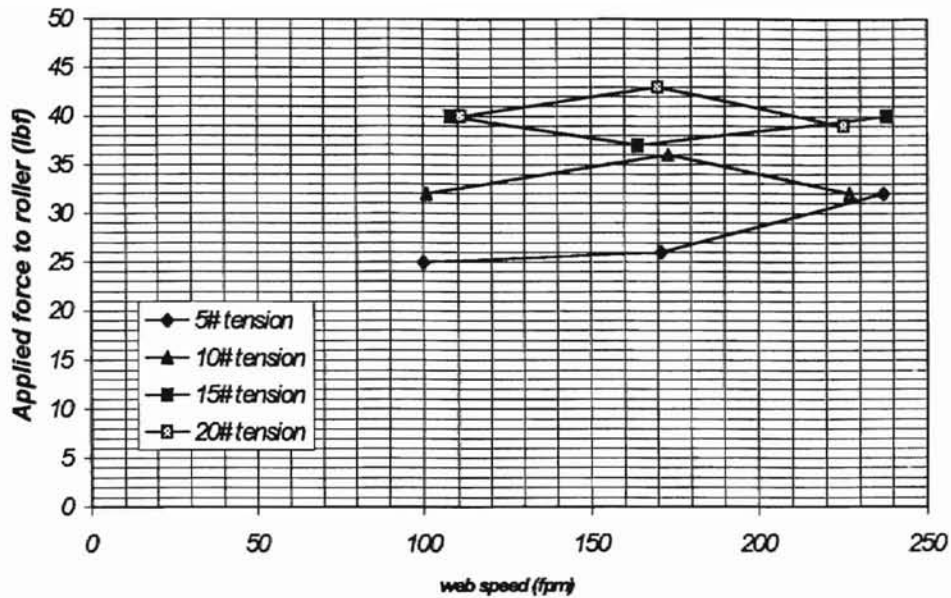
figure 21: Applied Force to cause Hard Crease Vs. Web Speed (18 gauge web, PET on MRT)

As can be seen from the previous plots certain trends are apparent. As the web caliper decreases the amount of force applied to the roller to reach a hard crease decreases also. In addition all of the curves to be grouped in the same vicinity on the charts. This seems to suggest that wrinkle formation in this case is not dependent on the web line tension.

The above experiments are repeated once again on the same web calipers however in this set the point of impending wrinkle, not a hard crease, is noted. It should be noted once more that the condition defining an "impending" wrinkle is subjective and that it was noticed that there is a slight transitional region of deflection where the wrinkle may be considered "impending". With this in mind a consistency in the behavior of a wrinkle where a data point was collected was attempted to be maintained. The results of this experimentation may be seen in figures 22, 23 and 24.
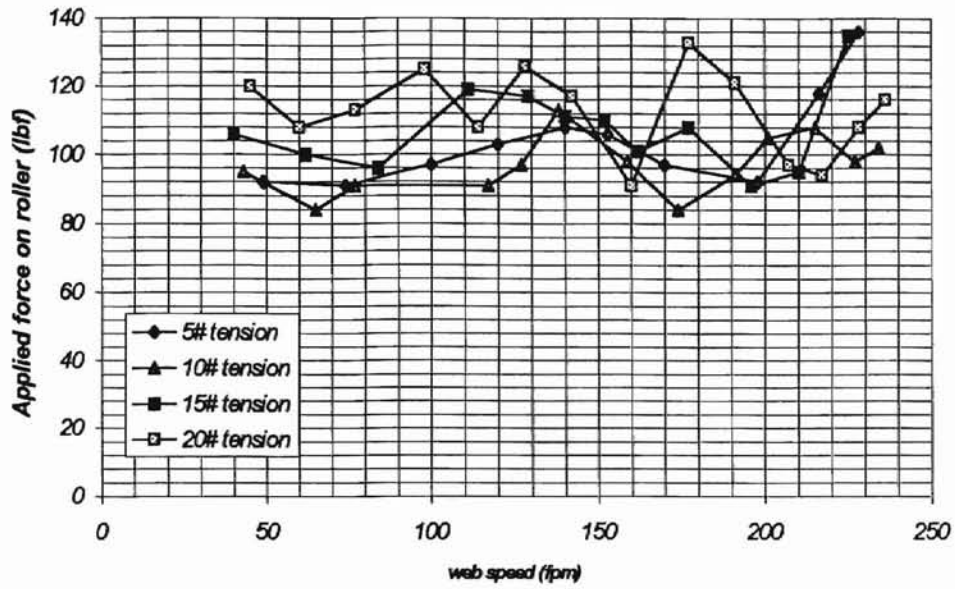
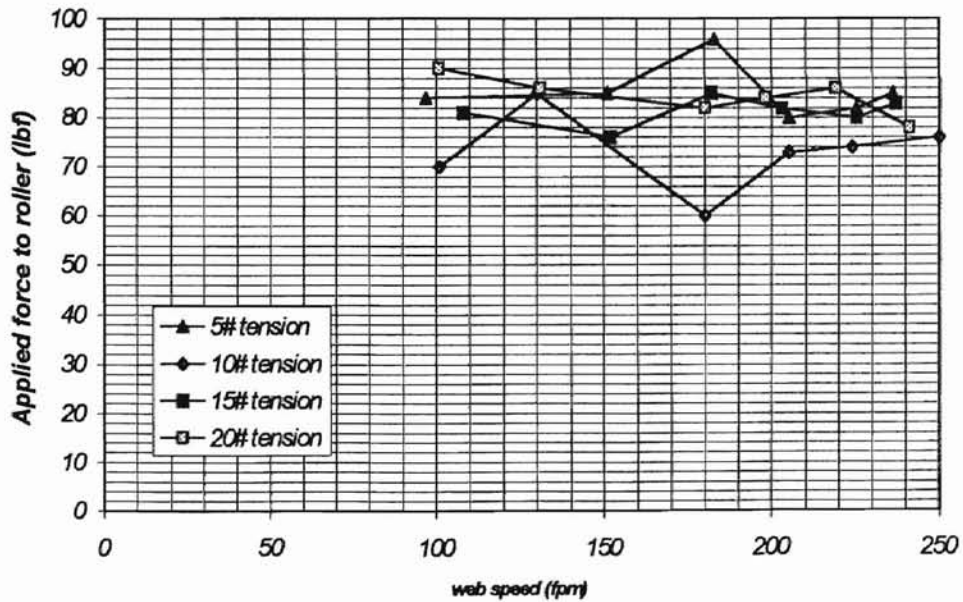figure 22: Force Applied to Cause Impending Wrinkle Vs. Web Speed (56 gauge web, PET on MRT)

figure 23: Applied Force to Cause Impending Wrinkle Vs. Web Speed (38 gauge web, PET on MRT)
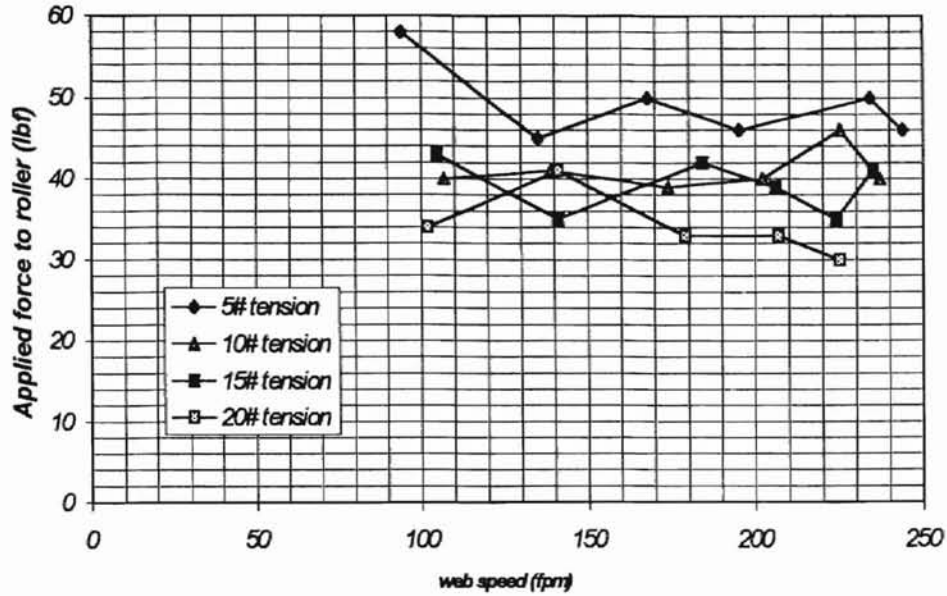
figure 24: Applied Force to Cause Impending Wrinkle Vs. Web Speed (26 gauge web, PET on MRT)

As can be seen in the above plots, some inconsistencies are present as in the first set of experiments. All of the applied forces decrease with the web caliper. Once again this is saying that the required amount of roller deflection to initiate a wrinkle is less for a thinner web. In addition the curves are all generally located in the same vicinity. This tends to suggest once again that the wrinkling effect is independent of the web tension. It can be noticed that the data for the impending wrinkle case appears to be a little more erratic on the plots. This may be explained by the mere fact that the impending wrinkle state is subjective and the point at which a wrinkle is determined to be "impending" may vary slightly.

VI.

Analysis of Experimental Results

The success of the previous experimentation to create a wrinkle at many different web line tensions and web line speeds is a partial. The initial purpose of this study was to analyze and experimentally verify Shelton's theory of buckling due to lateral forces cause by a deflecting roller. The case which has been examined here appears to have not behaved in this manner. This theory states essentially that all lateral strain imparted to the web is done by the kinematic steering due to the curvature of the roller and is in the entering span of the web before it even reaches the roller. It has been seen in this experimentation that this is simply not occurring and that another deciding parameter is causing the web wrinkle. The question which remains to be answered is what is the mechanism for the wrinkle if it is not kinematic steering.

Before theorizing on what causes the wrinkle it is very important to discuss how Shelton's theory is incorrect in this case. The lateral strain imparted to the web is given by equations 6 and 15,

$$\varepsilon = 2K_1 L, \qquad [6]$$

and

$$K_1 = \frac{4z_{\frac{W}{2}}}{W^2}. \qquad [15]$$

As a reminder L is the length of the free span, W is the width of the web, and $z_{w/2}$ is the deflection at the web edge relative to the center of the roller. Substituting the data taken

of applied force and web tension into the deflection equation 43 and applying the above

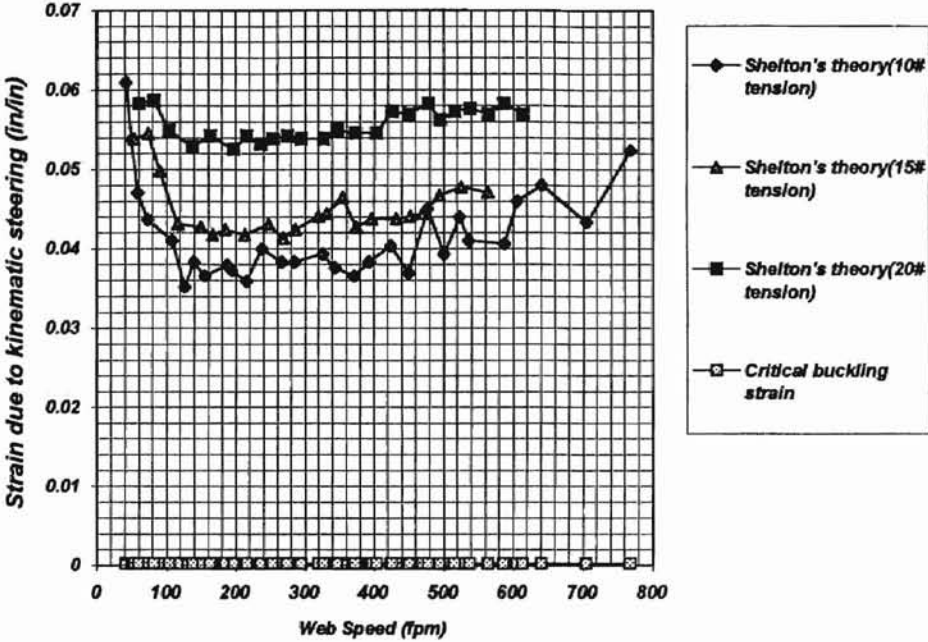kinematic strain equation allows for the generation of the following figures.

figure 25: Non-correlation of Shelton's theory and experimental points (48 gauge web, PET on aluminum)
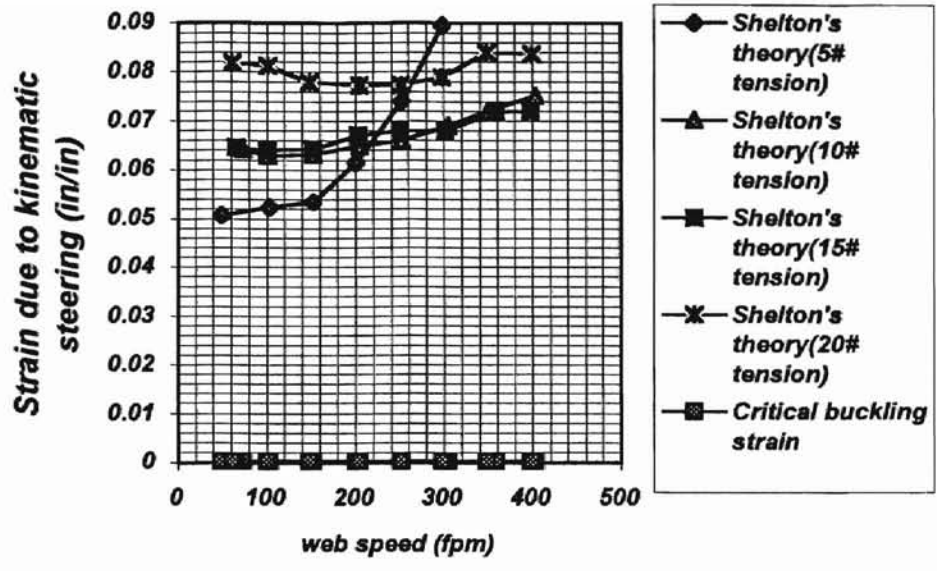
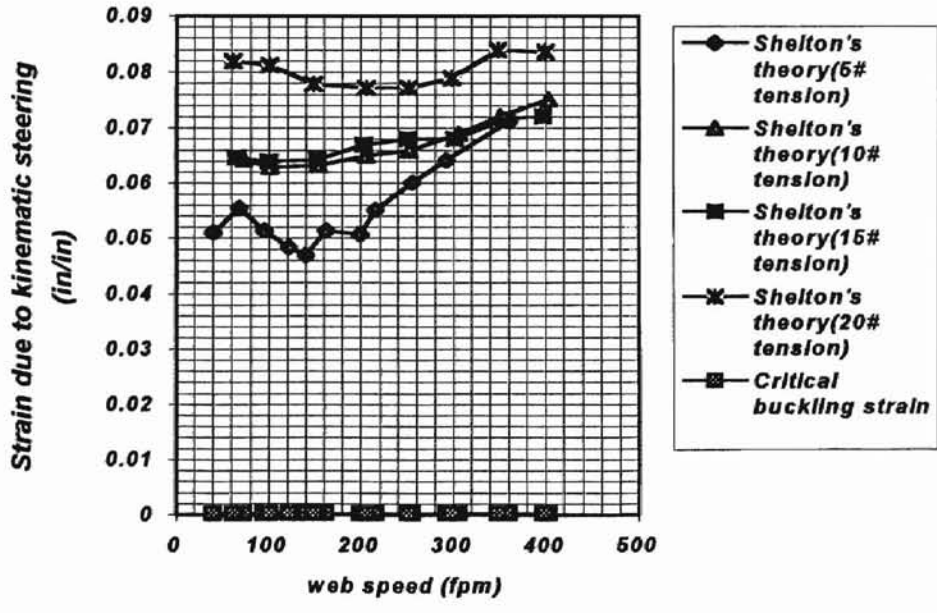figure 26: Non-correlation of Shelton's Theory to Experimental Data (48 gauge web, PET on MRT, hard wrinkle)

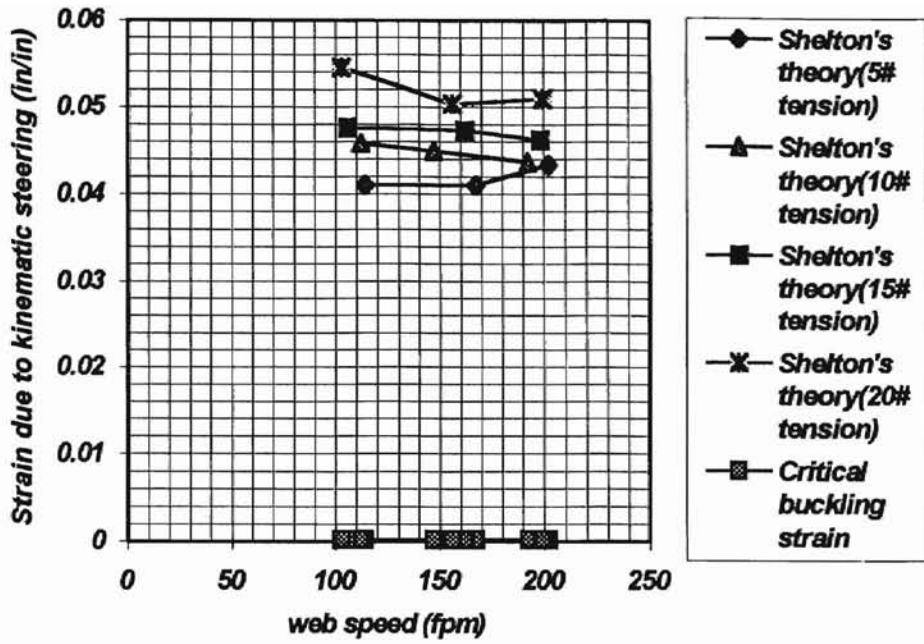figure 27: Non-correlation of Shelton's Theory to Experimental Data (56 gauge web, PET on MRT, hard crease)

figure 28: Non-correlation of Shelton's Theory to Experimental Data (38 gauge, PET on MRT, hard crease)
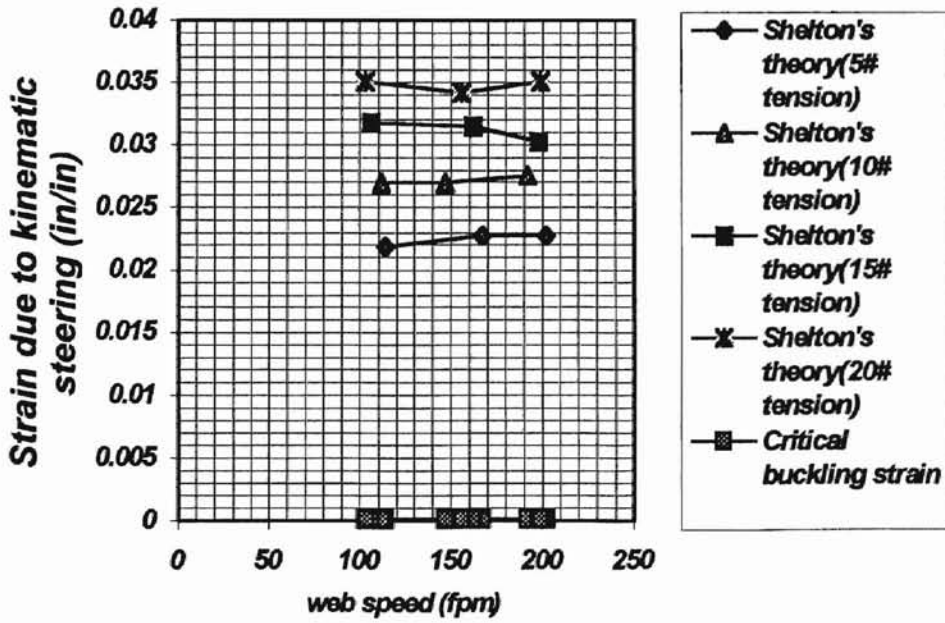

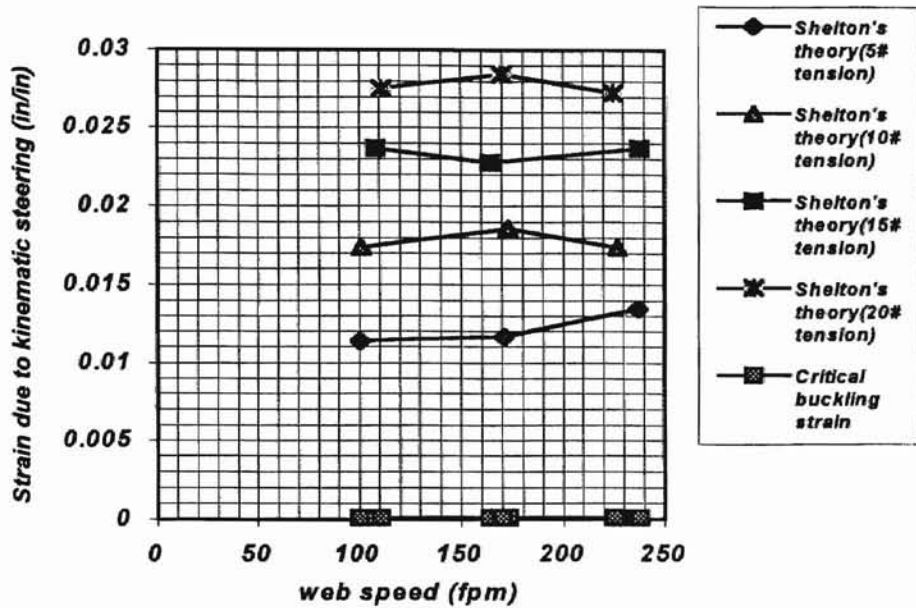Figure 29: Non-correlation of Shelton's Theory to Experimental data (26 gauge web, PET on MRT, hard crease)

figure 30: Non-correlation of Shelton's theory to experimental data (18 gauge web, PET on MRT, hard crease)
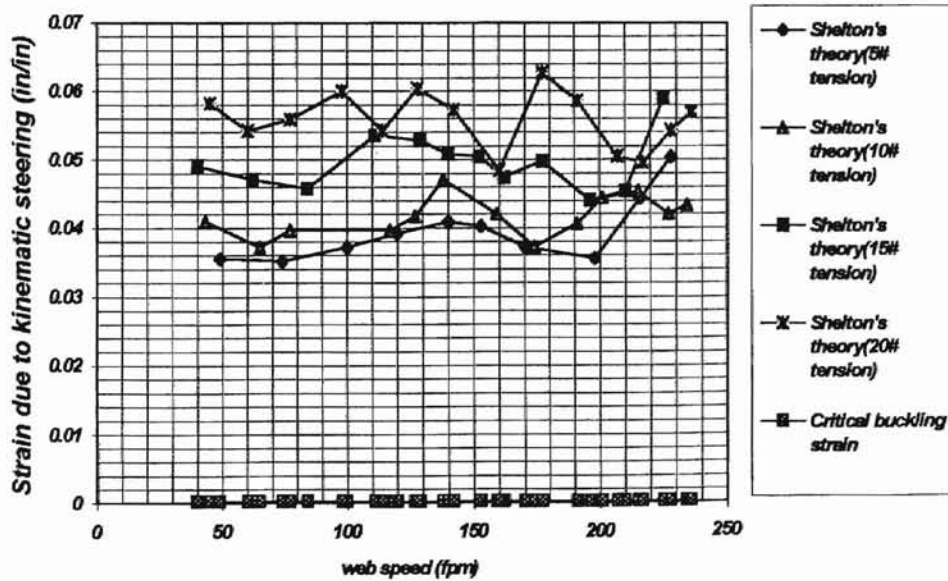

figure 31: Non-correlation of Shelton's Theory with Experimental Results (56 gauge web, PET on MRT, impending wrinkle)
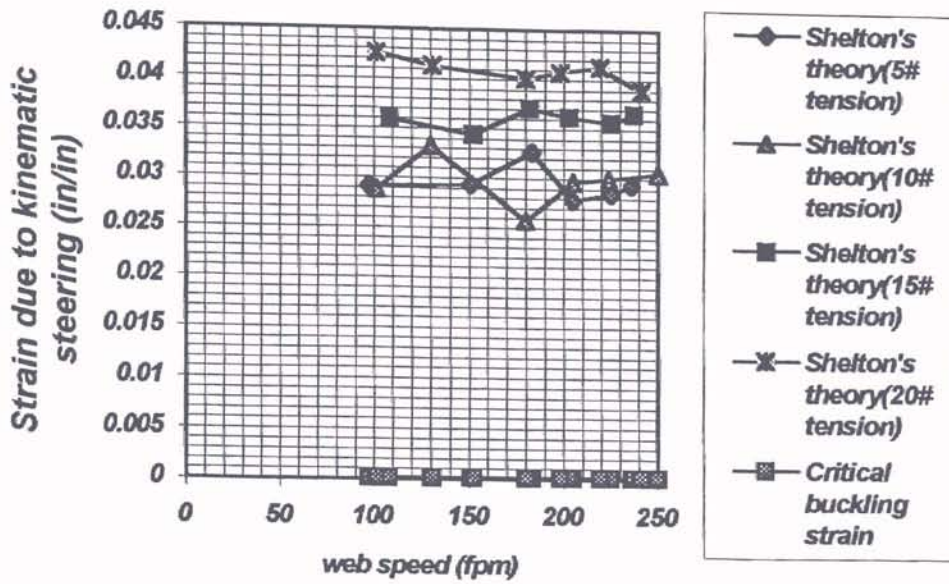
46

figure 32: Non-correlation of Shelton's Theory to Experimental data (38 gauge web, PET on MRT, impending wrinkle)
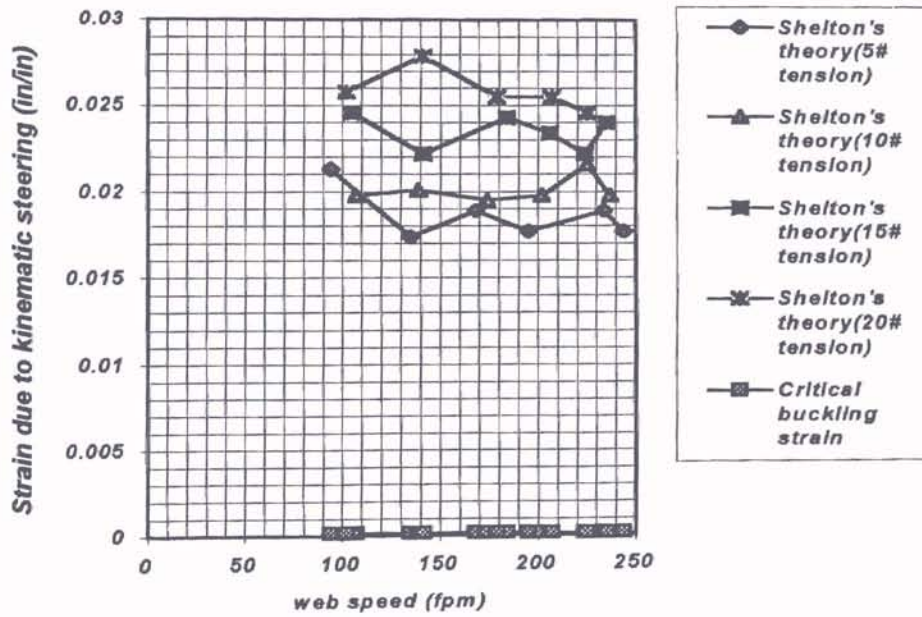

figure 33: Non-correlation of Shelton's Theory to Experimental Data (28 gauge web, PET on MRT, impending wrinkle)

As can be seen from the 9 previous figures, the strain induced due to kinematic steering at the deflections calculated by the derived deflection equation are extremely high in all cases, and should cause hard creases and wrinkles. Even the lowest value calculated, 0.02 in/in, seems outrageously high when speaking of a strain. The strains calculated due to steering in no way possible agree with the critical buckling strain of the film shell in contact with the roller.

The question still remains as to what is the mechanism for the wrinkling. The theory this study suggests is actually a quite simple one. If it is assumed that there is no slippage between the web and the roller, then the web simply undergoes the same strains as that of the roller. Simply stated, the bending strain on the surface of the roller in contact with the web is imparted to the web. The location of the maximum compressive strain due to bending is located on the top surface of the roller and may be found with the following relation

$$\varepsilon_{yy} = -z''(y)\frac{D_{out}}{2}. \quad [45]$$

The term z"(y) in equation 45 is the second derivative of the deflection equation and D_{out} is the outside diameter of the roller. Taking the second derivative of equation 43 and substituting the value 2.508" along with z"(y) allows for the formulation of a new set of figures relating the bending strain imparted to the web. These plots would display the strain in the web due to the film just conforming to the shape of the roller in its deflected form.
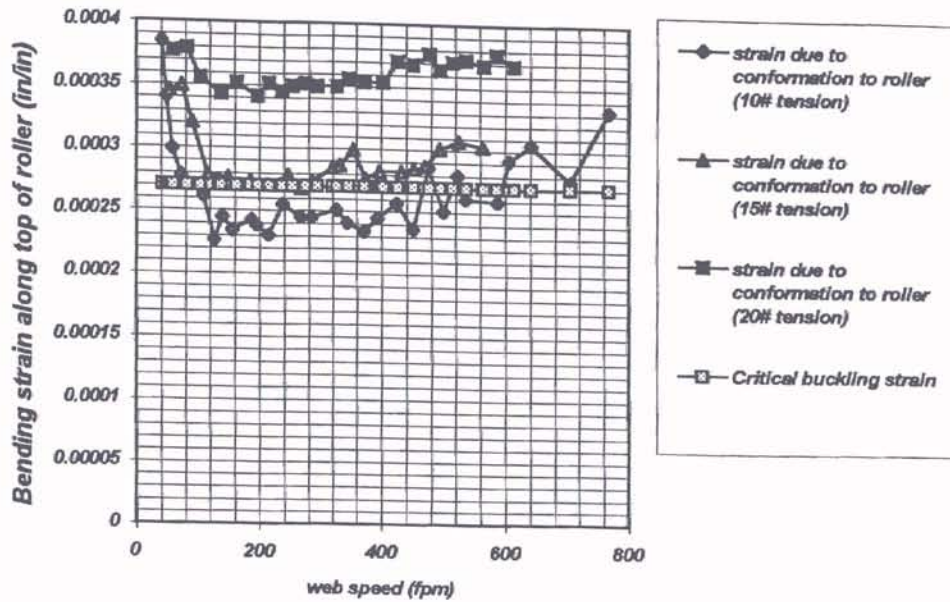
figure 34: Strain in Web Assuming Only Conformation to Roller Shape (48 gauge web, PET on aluminum, hard crease)
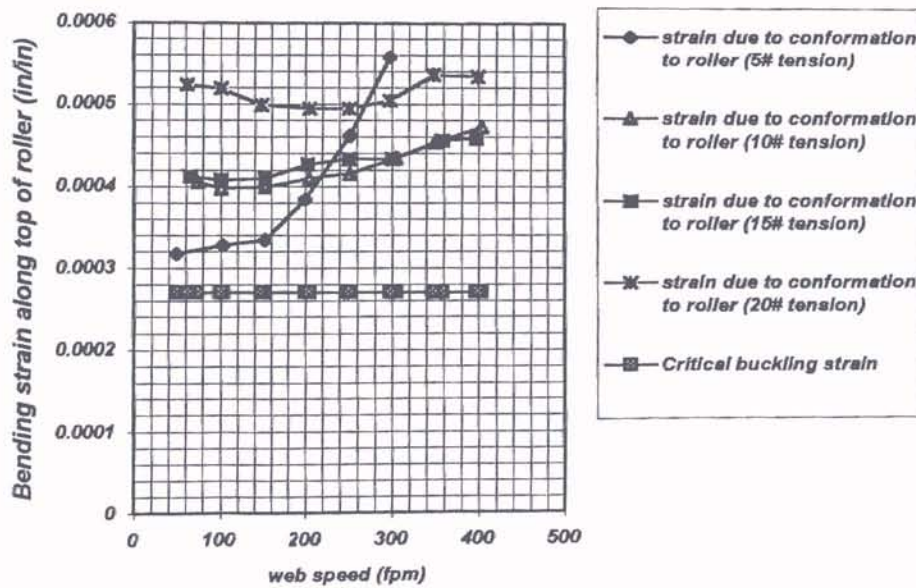

figure 35: Strain in Web Due to Conformation to Roller Deflection (48 gauge web, PET on MRT, hard wrinkle)
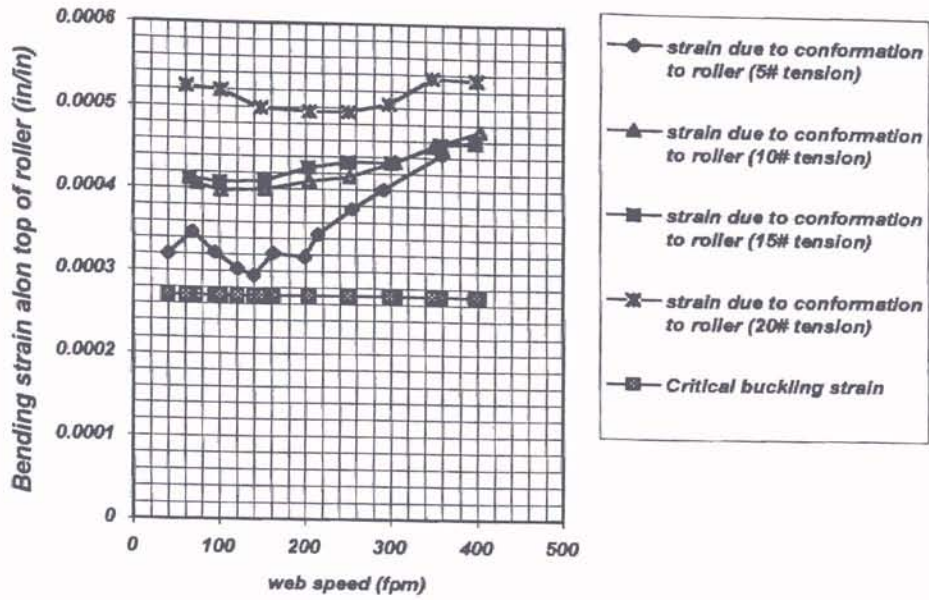
figure 36: Strain in Web Due to Conformation to Roller Deflection (56 gauge web, PET on MRT, hard crease)
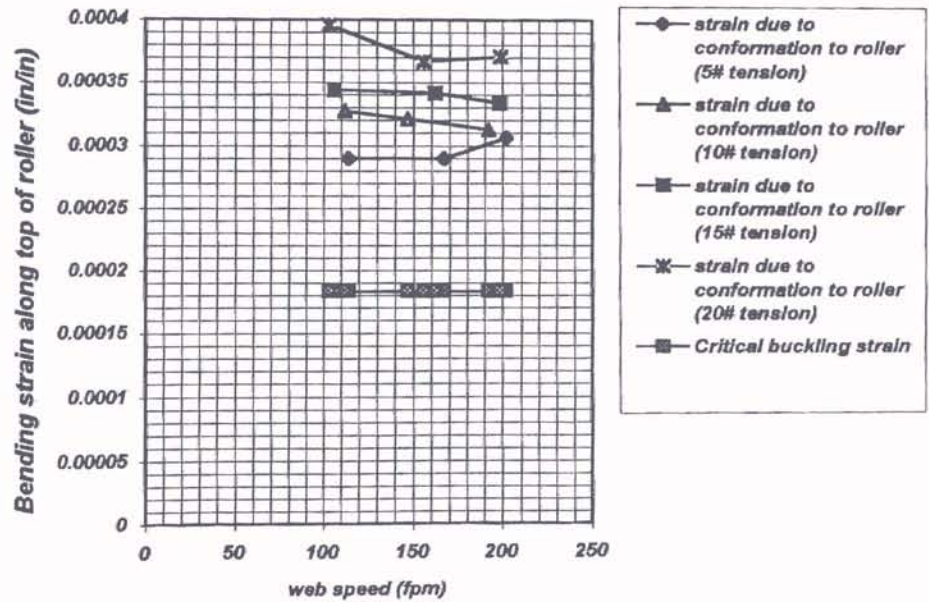

figure 37: Strain in Web Due to Conformation to Roller Deflection (38 gauge web, PET on MRT, hard crease)
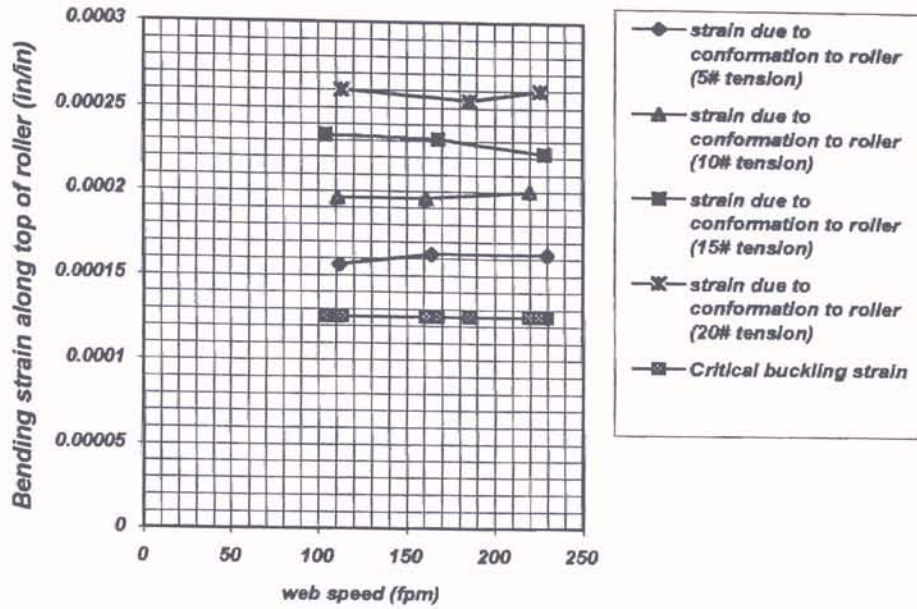
figure 38: Strain in Web Due to Conformation to Roller Deflection (26 gauge web, PET on MRT, hard crease)
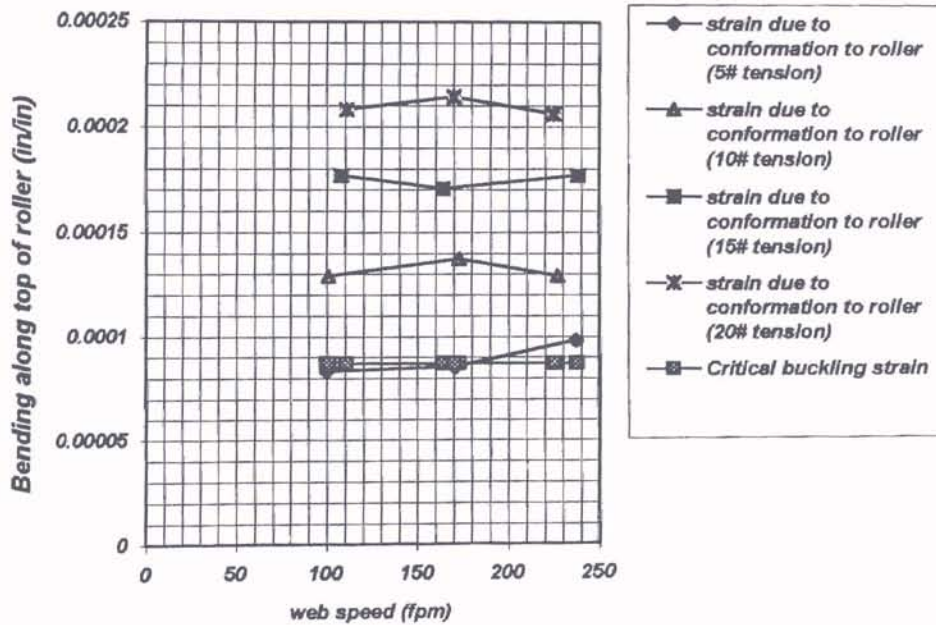

figure 39: Strain in Web Due to Conformation to Roller Deflection (18 gauge web, PET on MRT, hard crease)
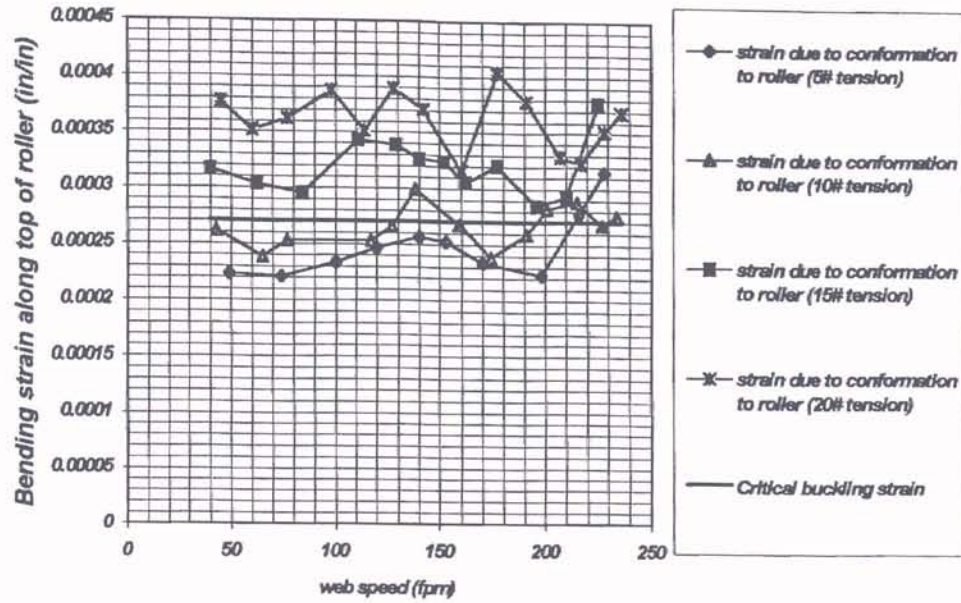
figure 40: Strain Due to Conformation to Roller Deflection (56 gauge web , PET on MRT, impending wrinkle)
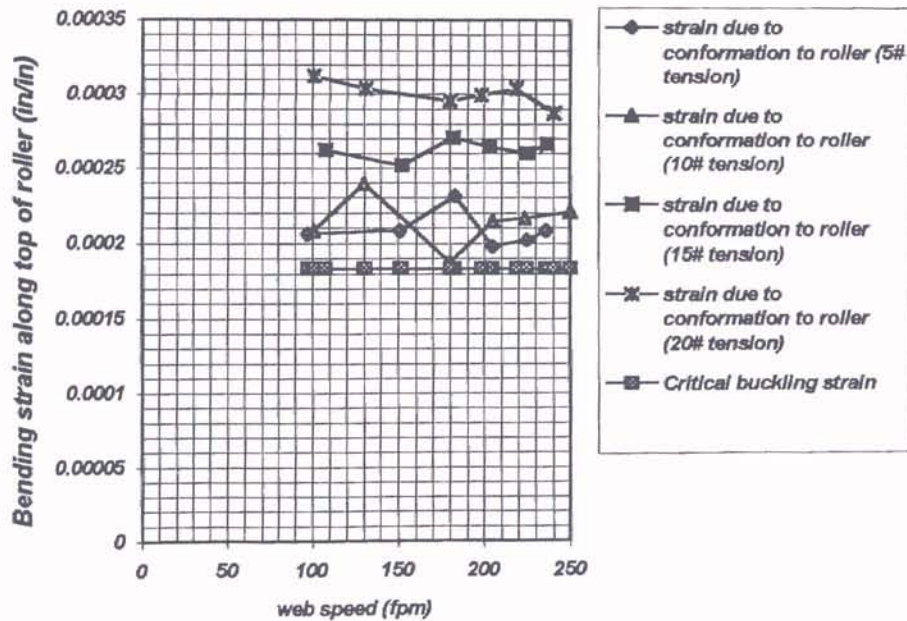

figure 41: Strain in Web Due to Conformation to Roller Deflection (38 gauge web, PET on MRT, impending wrinkle)
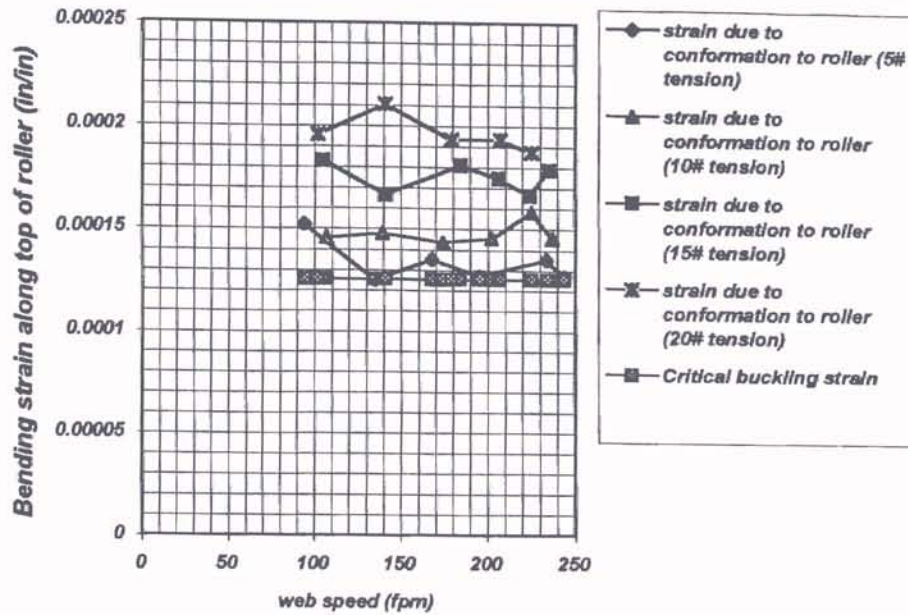
figure 42: Strain in Web Due to Conformation to Roller Deflection (28 gauge
web, PET on MRT, impending wrinkle)

As can be seen in the new figures, the assumption that the web takes on the same strain as

that of the deflecting roller agrees much better with the experimental results and with the

critical buckling strain model. The cases of best agreement are the tests where the

impending wrinkle formation is analyzed. Seen in figures 40 thru 42 are probably the best

correlations. While the hard crease data does in a way support the theory of the web

merely conforming to the shape of the deflected roller, the impending wrinkle does more

closely approximate a critical point being reached.

53

VII.

Conclusions and Recommendations

The initial purpose of this study was to design and build a working model supporting Shelton's theory of buckling due to lateral forces caused by a deflecting roller. The result however of this study was that the case examined actually did not obey the proposed theory. In this case a new theory was proposed in which the web merely assumes the shape of the deflected roller. In this way the strains which the roller undergoes in its deflection are imparted to the web. This is unlike the theory proposed by Shelton in which all strains are imparted to the web in the entering span before the web reaches the deflected roller. The first theory appears to be supported by experimental results and data. By no means is this study concluding that the initial lateral force theory is incorrect, it is merely stating that it did not hold for the one experimental case examined. The experiments documented in this study were only performed on a 6" wide web having a 180° angle of wrap around a deflecting roller and a 54" entering web span. It can be seen in equation 19 the effects that varying these parameters has on the inequality. It is my suggestion that the previous set of experiments be repeated with varying incoming web spans, web widths, and angle of wrap of the deflecting roller. It is only in this way that the entirety of this problem may be experimentally explored.

References

1) Good, J.K. and D.M. Kedl, "Predicting Shear Wrinkles in Web Spans", August 1989 <u>Tappi Journal</u>, pg. 1

2) Shelton, J.J., "Machine direction troughs in web spans and corrugations in wound rolls", Web Handling Research Center Oklahoma State University, project 8600-10, September 1991, pg. 3

3) Shelton, J.J., "Machine direction troughs in web spans and corrugations in wound rolls", Web Handling Research Center Oklahoma State University, project 8600-10, September 1991, pg. 2

4) Shelton, J.J., "Machine direction troughs in web spans and corrugations in wound rolls", Web Handling Research Center Oklahoma State University, project 8600-10, September 1991, pg. 12

5) Shelton, J.J., "Machine direction troughs in web spans and corrugations in wound rolls", Web Handling Research Center Oklahoma State University, project 8600-10, September 1991, pg. 14

6) Shelton, J.J., "Machine direction troughs in web spans and corrugations in wound rolls", Web Handling Research Center Oklahoma State University, project 8600-10, September 1991, pg. 17

7) Timoshenko & Gere, <u>Mechanics of Materials, 3rd edition</u>, 1984 Wadsworth, Inc. pg. 505.

8) Timoshenko & Gere, <u>Mechanics of Materials, 3rd edition</u>, 1984 Wadsworth, Inc. pg. 510.

9) Shelton, J.J., "Machine direction troughs in web spans and corrugations in wound rolls", Web Handling Research Center Oklahoma State University, project 8600-10, September 1991, pg. 16

10) Shelton, J.J., "Machine direction troughs in web spans and corrugations in wound rolls", Web Handling Research Center Oklahoma State University, project 8600-10, September 1991, pg. 18

11) Niordson, F.I., <u>Shell Theory</u>, Elsevier Science Publishers B.V. 1985 pg. 394

12) Timoshenko & Gere, <u>Mechanics of Materials, 3rd edition</u>, 1984 Wadsworth, Inc. pg. 761.

13) Van Vlack, Lawrence, <u>Elements of Material Science and Engineering, 6th edition,</u> Addison-Wesley, 1989, cover.

Bibliography

Langhaar, Henry L., <u>Energy Methods in Applied Mechanics,</u> Drieger Publishing Company Malabar, Florida, 1962

Narayanan, R. <u>Shell Structures,</u> Elsevier Applied Science Publishers LTD 1985.

Vinson, Jack R., <u>Structural Mechanics: The Behavior of Plates and Shells,</u> John Wiley & sons Inc. 1974.

Timoshenko, S., <u>Theory of Plates and Shells,</u> Mcgraw Hill, 1940.

Calladine, C.R., <u>Theory of Shell Structures,</u> Cambrige University Press, 1983.

VITA

Matthew G. Duvall

Candidate for the Degree of

Master of Science

Thesis: A STUDY OF WEB WRINKLING DUE TO ROLLER CURVATURE

Major Field: Mechanical Engineering

Biographical:

  Personal Data: Born in Okmulgee, Oklahoma, on October 19, 1971, the son of
  Darel Duvall and Marcy Mullings.

  Education: Graduated from Putnam City North High School, Oklahoma City,
  Oklahoma in may 1989; received Bachelor of Science degree in Mechanical
  Engineering from Oklahoma State University, Stillwater, Oklahoma in
  December of 1994. Completed the requirements for the Master of Science
  degree with a major in Mechanical Engineering at Oklahoma State
  University in (May, 1997).

  Experience: Employed as a construction laborer in summers; employed by
  Oklahoma State University, school of Mechanical Engineering as a
  teaching assistant; employed by Oklahoma State University, Web Handling
  Research Center as a graduate research assistant.